LEVEL II

Technical Report
on

Application of Surface Analysis Techniques to Pulsed Power Problems
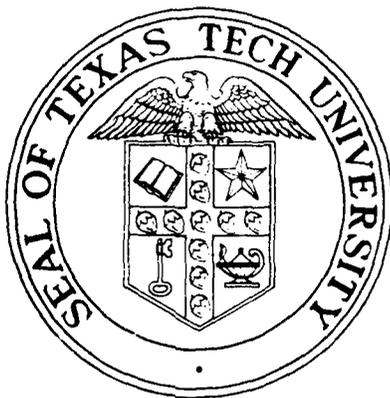
by
G. L. Jackson

March 23, 1981

DTIC
ELECTE
JUL 7 1981

F

PLASMA AND SWITCHING LABORATORY
LASER LABORATORY

DEPARTMENT OF ELECTRICAL ENGINEERING

TEXAS TECH UNIVERSITY

Lubbock, Texas 79409

81 7 06 119

REPORT DOCUMENTATION PAGE	READ INSTRUCTIONS BEFORE COMPLETING FORM
1. REPORT NUMBER AFOSR-TR- 81 - 0501	2. GOVT ACCESSION NO. AD-A100 971	3. RECIPIENT'S CATALOG NUMBER

4. TITLE (and Subtitle) Application of Surface Analysis Techniques to Pulsed Power Problems	5. TYPE OF REPORT & PERIOD COVERED *INTERIM*
	6. PERFORMING ORG. REPORT NUMBER

7. AUTHOR(s) G.L. Jackson	8. CONTRACT OR GRANT NUMBER(s) F49620-79-C-0191

9. PERFORMING ORGANIZATION NAME AND ADDRESS Dept. of Physics and Dept. of Electrical Engineering, Texas Tech University, P.O. Box 4180 Lubbock, Texas 79409	10. PROGRAM ELEMENT, PROJECT, TASK AREA & WORK UNIT NUMBERS 2301A7 61102F
11. CONTROLLING OFFICE NAME AND ADDRESS AFOSR/NP Bolling AFB Wash DC 20332	12. REPORT DATE 3/23/81
	13. NUMBER OF PAGES 134
14. MONITORING AGENCY NAME & ADDRESS(if different from Controlling Office)	15. SECURITY CLASS. (of this report) Unclassified
	15a. DECLASSIFICATION/DOWNGRADING SCHEDULE

16. DISTRIBUTION STATEMENT (of this Report)

Approved for public release;
distribution unlimited.

17. DISTRIBUTION STATEMENT (of the abstract entered in Block 20, if different from Report)

18. SUPPLEMENTARY NOTES

19. KEY WORDS (Continue on reverse side if necessary and identify by block number)

Insulators, Electrodes, Polymers, UV damage, Surface analysis, Pulsed Power

20. ABSTRACT (Continue on reverse side if necessary and identify by block number)

An assessment of some of the advantages and disadvantages of various surface analysis techniques applied to the analysis of both the insulators and conductors used in high voltage spark gaps is presented. Some of the analysis techniques introduced include Electron Spectroscopy for Chemical Analysis, Auger Electron Spectroscopy, X-ray Fluorescence, and Secondary Ion Mass Spectroscopy. The purpose of this review is to present some of these analysis techniques with emphasis placed on those techniques which give information about changes that occur on or near the surfaces of insulators and conductors. Surface charging makes most

DD FORM 1473 EDITION OF 1 NOV 65 IS OBSOLETE

analysis techniques incapable of giving useful information about the changes on
or near the surface of insulators. Because of the amount of information avail-
able from a single ESCA spectrum, such as shifts in binding energies due to
changes in chemical environment, Auger electron peaks due to the relaxation of
the atom after photoionization, and the quantitative information, ESCA is the
best analysis technique available for the investigation of insulators. Also
the problem of surface charging in ESCA is minimal. The analysis of conductors,
however, is less complicated because surface charging is no longer a problem.
Therefore, the use of AES, SIMS, and ESCA can all give some useful information
about conductor surfaces. Since there are several damage mechanisms involved
in the deterioration of high voltage spark gaps, such as ultraviolet radiation
from the arc, heat from the arc, emission of microparticles from the electrodes,
and chemically reactive species in gas filled gaps, it is necessary to try to
eliminate as many parameters as possible in order to better understand the
damage caused by each mechanism. Therefore, a vacuum chamber has been built
whereby the damage caused by ultraviolet radiation can be separated from the
damage caused by other mechanisms. Insulator samples are radiated with ultra-
violet radiation and the samples are then analyzed with appropriate surface
analysis techniques to determine what, if any, changes the exposure to the
radiation caused.

Application of Surface Analysis

Techniques to Pulsed Power Problems.

by

G.L. /Jackson

Mar̶̶̶81

Technical Report No. 1 on

AFOSR Contract/ F49620-79-C-0191

"Coordinated Research Program in
Pulsed Power Physics"

Project No. 4

"Pulsed Power Surface Physics
and Applications"

$PP-1$

Principal Investigator:
L.L. Hatfield
Associate Professor

Co-Principal Investigator:
M. Kristiansen
P.W. Horn Professor

Plasma and Switching Laboratory
Department of Electrical Engineering
and
Department of Physics
Texas Tech University
Lubbock, Texas 79409

TABLE OF CONTENTS

Abstract

List of Tables

List of Figures

i

Acknowledgments

ABSTRACT

An assessment of some of the advantages and disadvantages of various surface analysis techniques applied to the analysis of both the insulators and conductors used in high voltage spark gaps is presented. Some of the analysis techniques introduced include Electron Spectroscopy for Chemical Analysis, Auger Electron Spectroscopy, X-ray Fluorescence, and Secondary Ion Mass Spectroscopy. The purpose of this review is to present some of these analysis techniques with emphasis placed on those techniques which give information about changes that occur on or near the surfaces of insulators and conductors. Surface charging makes most analysis techniques incapable of giving useful information about the changes on or near the surface of insulators. Because of the amount of information available from a single ESCA spectrum, such as shifts in binding energies due to changes in chemical environment, Auger electron peaks due to the relaxation of the atom after photoionization, and the quantitative information, ESCA is the best analysis technique available for the investigation of insulators. Also the problem of surface charging in ESCA is minimal. The analysis of conductors, however, is less complicated because surface charging is no longer a problem. Therefore the use of AES, SIMS, and ESCA can all give some useful information about conductor surfaces. Since there are several damage mechanisms involved in the deterioration of high voltage spark gaps, such as ultraviolet radiation from the arc, heat from the arc, emission of microparticles from the electrodes, and chemically reactive species in gas filled gaps, it is necessary to try to eliminate as many para-

iii

meters as possible in order to better understand the damage caused by each mechanism. Therefore a vacuum chamber has been built whereby the damage caused by ultraviolet radiation can be separated from the damage caused by other mechanisms. Insulator samples are radiated with ultraviolet radiation and the samples are then analyzed with appropriate surface analysis techniques to determine what, if any, changes the exposure to the radiation caused.

LIST OF TABLES

LIST OF FIGURES

Chapter 1

Introduction

In pulsed power technology, little is known about the basic
physical processes responsible for damage to insulators and con-
ductors used in high voltage spark gaps. The generation of ultra-
violet photons in the arc, microparticles from the surface of elec-
trodes, and chemical effects on insulators and electrodes in gas fill-
ed gaps are mechanisms that can cause changes and/or damage to the
various parts of spark gaps. The purpose of this report is to review
some of the major techniques available that can give useful informa-
tion about some of the changes that occur on or near the surfaces of
insulators and conductors. The main objective is to select one or
more of these techniques for the investigation of the surfaces of in-
sulators and conductors.

Some of the changes that can occur on the surfaces of insulators
are changes in crosslinking patterns, elemental composition changes,
and the implantation of microparticles from the electrodes, result-
ing in a possible change of conductivity of the insulator. Cross-
linking is the interbonding of chains of molecules in a polymer.
Changes in the crosslinking pattern of a polymer, due to the break-
ing of bonds in the polymer chain and subsequent reorganization,
can result in stresses and strains to the polymer. Elemental com-
position changes result from the loss of atoms from the surface due
to sputtering. The sputtering of particles from the surface can re-
sult from either physical or chemical processes. Physical sputter-
ing is the process by which a transfer of kinetic energy from inci-
dent particles on the surface results in the ejection of particles.

However, only those particles with sufficient kinetic energy to overcome the binding forces of the surface will be ejected. Chemical sputtering is the process by which a chemical reaction is induced on the surface in the presence of a reactive gas, resulting in the formation of chemical compounds. The compound formation can cause lowering of the binding forces of the surface, resulting in the ejection of molecular species from the surface. Both of these sputtering processes will change the elemental composition of the surface. The implantation of microparticles on the insulator surface causes sputtering away of the surface material and it may change the conductivity of the surface by introducing highly conductive particles to the surface.

On conductors, similar processes can occur. For example, the elemental composition of the surface can change through chemical sputtering processes. The matrix of the conductor may be changed by the emission of microparticles from the surface or by the interaction of the surface with the surrounding gas in gas filled gaps.

The analysis techniques with their common acroymns, which will be be introduced in this review, are listed in Table 1-1. These techniques by no means exhaust the list of analytical techniques available, however each of these techniques has one or more characteristics that make it attractive for the investigation of surface phenomena. Information about each technique will be presented in order that a better understanding of the technqiue can be achieved. After a basic description of all these techniques, an assessment of the different techniques will be presented and a set of criteria such as the detection of all elements present in the material, quant-

Table 1-1

Surface Analysis Techniques

ESCA   Electron Spectroscopy for Chemical Analysis

AES   Auger Electron Spectroscopy

SIMS   Secondary Ion Mass Spectroscopy

ISS   Ion Scattering Spectroscopy

PAS   Photoacoustic Spectroscopy

ATR   Attenuated Total Reflection

SEM   Scanning Electron Microscopy

SIPS   Sputter Induced Photon Spectroscopy

Other Techniques:

   Optical Microscopy

   Profilometry

   Surface Resistivity

   Ellipsometry

itative analysis, analysis of chemical changes, depth of analysis,

and ease of analysis will be chosen in order to decide which ana-

lytical techniques are best suited for the problems at hand.

Before a discussion of these analytical techniques can begin,

an understanding of what makes up a surface is mandatory. By defi-

nition, a surface is an interface, a marked discontinuity between one

material and another or between one phase and another (liquid, gas,

solid, or plasma). What is meant by the depth of a surface depends

almost entirely upon the analytical technique to be employed as well

as the material itself. Figure 1-1 shows the depth distribution of

various forms of radiation in a material. In this figure the analy-

sis depth of ESCA, AES, and XRF are compared. This figure shows that

the depth from which Auger electrons can escape without loss of energy

is approximately 10 Å. It also shows that secondary electrons can es-

cape without loss of energy from a depth of approximately 50-500 Å.

Finally, it shows that characteristics x-rays can escape from approxi-

mately 10,000-20,000 Å deep in a material. Consequently, Fig. 1-1

shows that the depth of analysis depends upon the specific analysis

technique being used. Throughout the discussion of the various tech-

niques, the depth of analysis will be a critical parameter in the sel-

ection of the appropriate analysis technique.

As was mentioned earlier, some of the events that occur in high

voltage spark gaps, leading to the eventual destruction of the consti-

tuent parts of the spark gaps, are: emission of radiation from the arc

and surrounding gas, electrode sputtering, thermal and mechanical

shocks, and chemical bombardment of surfaces in gas filled gaps. Ob-
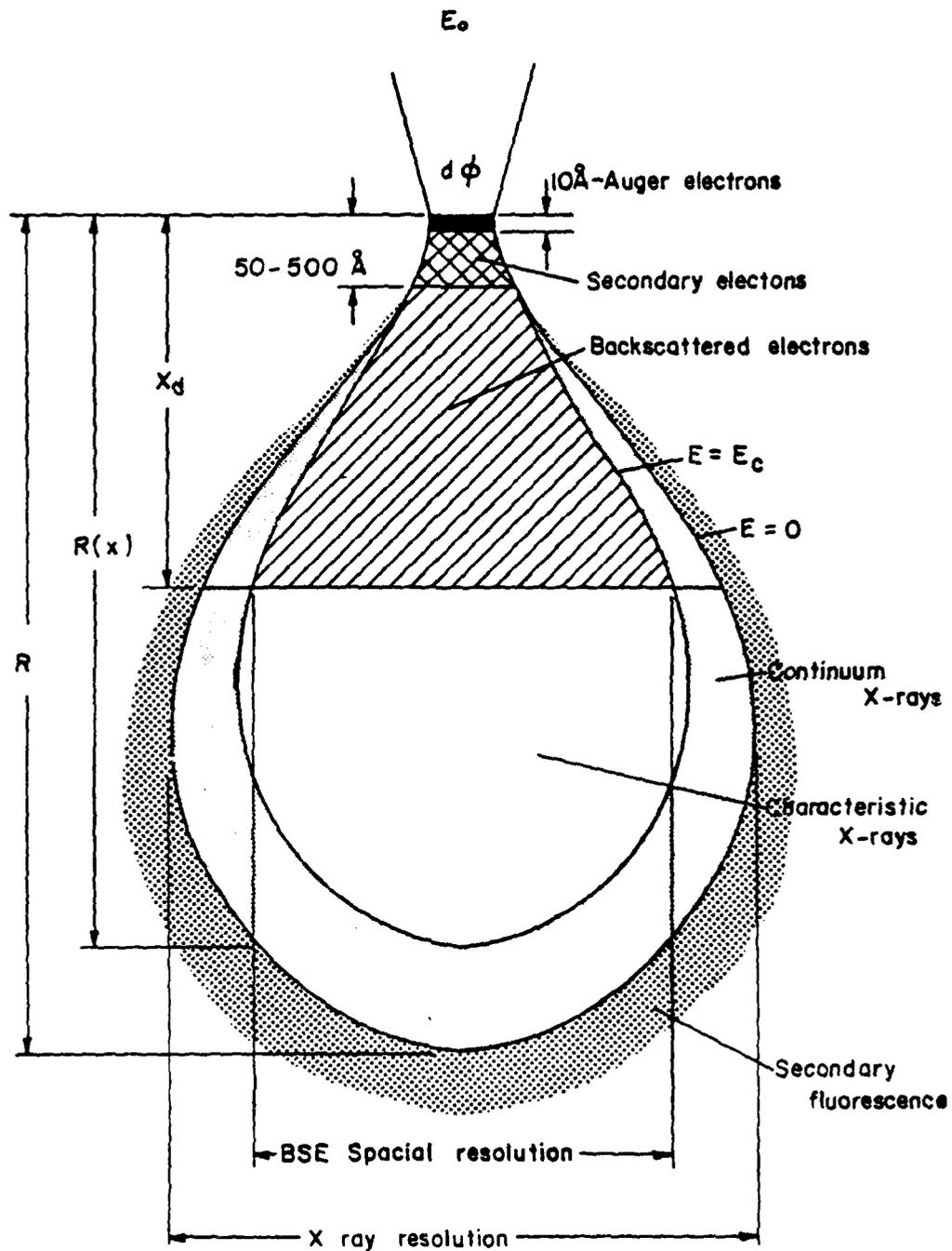
Figure 1-1 Analysis depth of AES, ESCA, and XRF. R is
approximately 3-5 um, and R(x) is approxi-
mately 1-2 um, and x_d is about .5 um.

viously, each mechanism has its own way of affecting the various surfaces of interest, therefore it is advantageous to try to separate and study these various mechanisms. With this objective in mind, an investigation into the effects of ultraviolet radiation on common insulators used in spark gaps has been initiated. A vacuum chamber has been built whereby the effects of ultraviolet light on insulators may be singled out from the other damage mechanisms. Before and after an insulator has been exposed to the radiation a study of its electrical resistivity and surface flashover potential is made. Also, each insulator will be tested with some of the above mentioned analytical tools for the purpose of determining what, if any, changes occurred to the material due to the ultraviolet radiation.

In summary, a partial introduction of surface analytical techniques will be presented with the objective of selecting an analytical technique suitable for the investigation of changes caused by various damage mechanisms or combinations of mechanisms.

Chapter 2

Electron Spectroscopy for Chemical Analysis (ESCA)

Electron Spectroscopy for Chemical Analysis [1,2,3,4] is per-
haps the most versatile analytical tehnique in common use for the
study of structure and bonding in organic and inorganic insulators.
It is also one of the top techniques for the analysis of conductors,
along with AES, ISS, SIMS and XRF. The acronym ESCA is the most
common; however, the technique is also commonly known as x-ray photo-
electron spectroscopy, UPS, and photoelectron spectroscopy, PES. In
this report the acroynm ESCA will be used to identify the technique,
unless otherwise indicated.

In the ESCA experiment a monochromatic beam of x-rays, usually
Al $K_{\alpha1,2}$ or Mg $K_{\alpha1,2}$ lines (with energies of 1486.6 eV and 1253.7
eV, respectively), is incident on the material to be analyzed. Be-
cause of the incident x-ray flux, photoelectrons from the core atomic
levels are ejected from the material with certain characteristic en-
ergies. The energy is characteristic of the element and related to
the binding energy of the ionized element and the energy of the inci-
dent radiation. The relationship between the measured kinetic
energy of the ejected electron and the calculated binding energies is
shown in Figure 2-1. [5]

The energy of the incident x-ray photon, $h\gamma$, is given to a core
electron. If the core electron has been given sufficient energy to be
promoted from its core level to a free electron state above the matrix
of the material, then the measured energy will be the kinetic energy
of the electron after taking into consideration the binding energy
and work function of the material. Also because of the conservation

7

$$h\nu = E_b + \phi_{sp} + T_{sp} + E_r$$
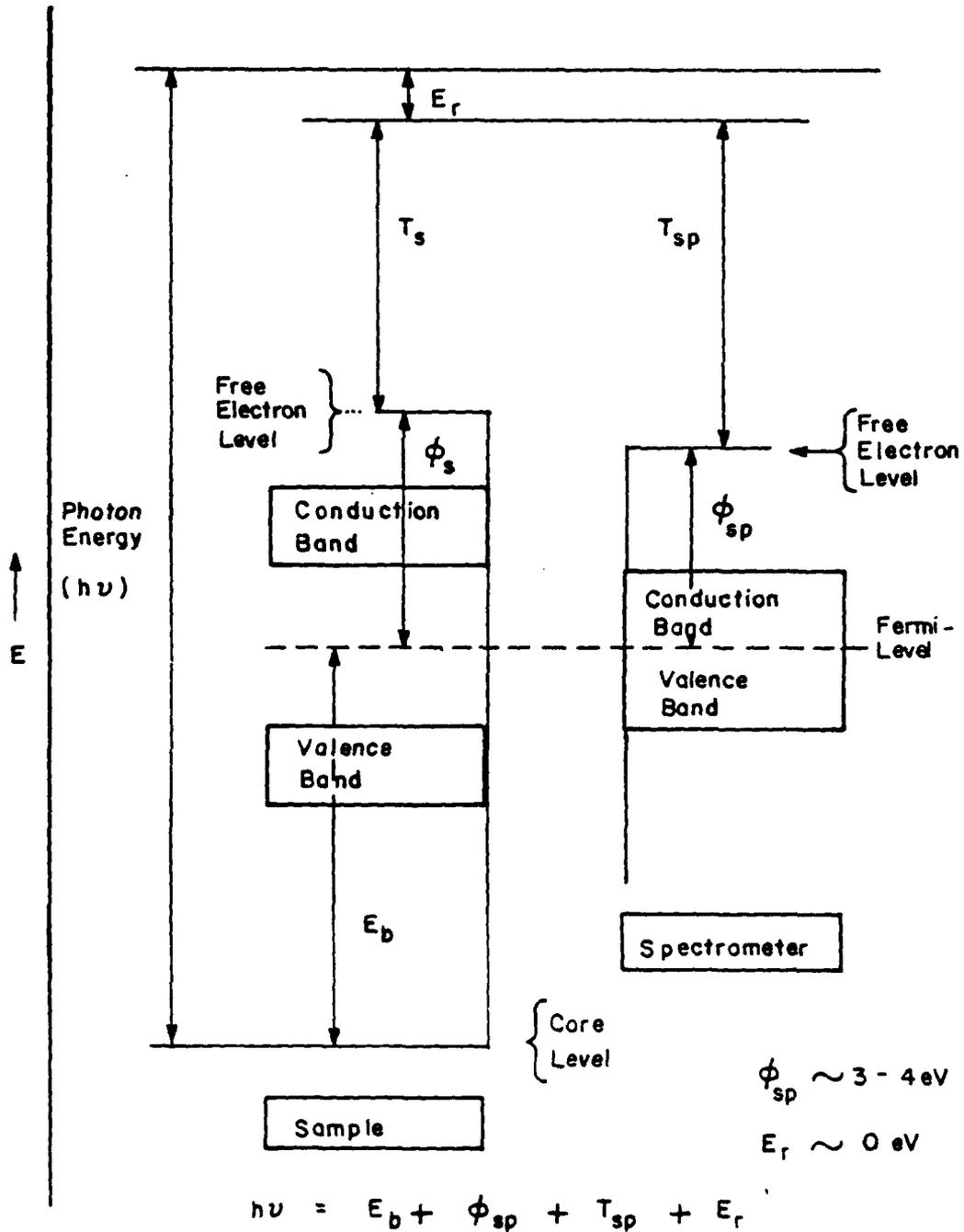
Figure 2-1 Energetics of electron-binding measurements in solids. All symbols are explained in text. (ref. 5).

of momentum, a small amount of energy will be imparted to the recoil. The recoil energy is a function of the atomic number and the energy of the exciting radiation. For lower atomic number elements the recoil energy is usually negligible.

When the ejected electron enters the spectrometer there are additional factors which must be considered. For example, when two materials are in electrical contact, as is to be the case for the sample and the spectrometer, the Fermi energies are at a common level. As the electron travels from the sample material to the exit slit it encounters a potential gradient due to the differences in work functions of the sample material and the spectrometer, experiencing an acceleration or deceleration to a kinetic energy, T_{sp}, as it reaches the free electron level of the spectrometer. Therefore the measured kinetic energy, T_{sp}, is given by

$$T_{sp} = h\nu - E_b - \phi_{sp} - E_r \tag{1}$$

To calculate the absolute binding energy of the core electron, E_b, the work function of the spectrometer, ϕ_{sp}, must be known accurately, assuming that the recoil energy, E_r, is negligible. However, in most instances absolute ginding energies are not required, but rather relative differences in binding energies.

The removal of the core electron is accompanied by a reorganization of the valence level of the material because of the effective increase in the nuclear charge seen by the valence electrons. When this reorganization occurs there is a finite probability for the excitation of a valence electron from an occupied state to an unoccupied state (shake-up), or the ionization of a valence electron (shake-off).

These shake-up and shake-off lines lie on the low energy side of the
main photoelectron peak and are usually of considerably less inten-
sity than the main photoelectron peak. Shake-up and shake-off lines
are shown in Fig. 2-2[2]. Their presence in the spectrum may give
considerable details about the structure and bonding in materials
once they are better understood.

Another interesting consequence of the ESCA experiment is the
appearance of Auger line energies in the spectrum. Because of the
core level vacancy after x-ray ionization there is a finite probability
for deexcitation of the ionized atom via either x-ray fluorescence or
Auger electron emission. Since the spectrometer measures the kinetic
energy of electrons emitted from the material, the Auger lines are
present in the ESCA spectrum and are independent of the energy of the
ionizing radiation used. Because the energies of Auger electrons are
characteristic of the element emitting the electron, the Auger lines
can be used to help make both qualitative and quantitative analysis of
the material. However, the analysis of materials by Auger electrons
is a subject that will be covered in another chapter of this report.

The basic advantages of ESCA as a surface analysis technique
compared with others, such as SIMS, AES, ISS, and XRF are:

1)   Because the x-ray fluxes used in conventional
     spectrometers are small there is no appreciable
     amount of damage done to the surface in the time
     it takes to perform the experiment. Therefore
     ESCA is basically a nondestructive technique com-
     pared with other techniques that employ electron or
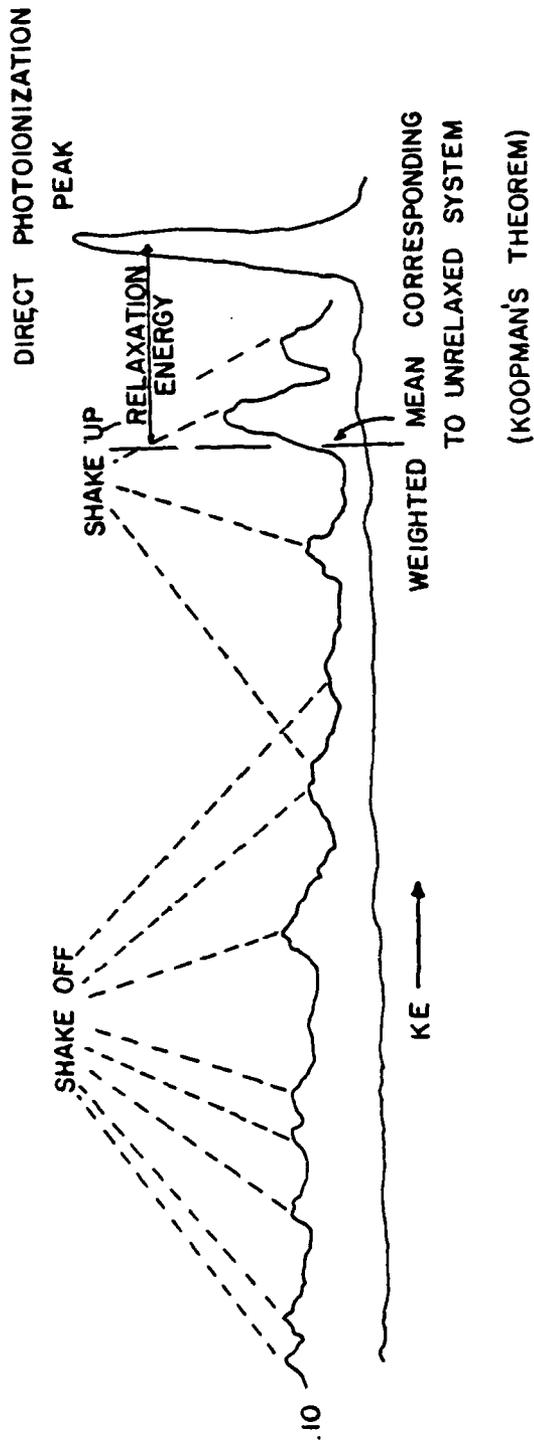
Figure 2-2 Relationship between relaxation energies, Koopman's Theorem and the relative intensities of direct photoionization and shakeup and shakeoff transitions. (ref. 2).

ion beams as the incident radiation.

2) The technique is highly sensitive to all elements, with the exception of hydrogen and helium. However, the cross-section for ionization of all elements by x-rays is not the same and therefore the sensitivity of ESCA is not the same for all elements.

3) The amount of information from a single spectrum is greater than from any other analytical technique. Absolute binding energies, relative peak intensities, shifts in binding energies, shake-up and shake-off satellites, multiplet splitting effects, and angular dependent studies which give depth profiling are all pieces of information readily available from an ESCA spectrum.

4) The depth of analysis is approximately 50-100 Å for polymeric insulators, consequently the depth of analysis is such that the first few molecular layers may be analyzed without bulk interactions.

5) Information can be obtained on both the core and valence energy levels of molecules.

6) Finally, the sample requirement is modest, for most cases 1 mg of the solid is all that is required.

The interpretation of the photoelectron spectrum is not always straightforward. Many factors influence both qualitative and quantitative analysis by ESCA. One of the most frustrating problems is that of surface charging in insulators. When an x-ray beam causes

emission of photoelectrons from the surface, the material gains a net positive charge due to the loss of electrons from the surface. The charging of the surface leads to an apparent increase in the binding energy, calculated by Eq. 1. There have been many attempts to correct the problem of surface charging; however, accurate corrections to the calculated binding energies because of sample charging are extremely complicated.

One method used to overcome surface charging problems is to calibrate the energy scale of the spectrometer using an external standard. If an insulating sample is not in electrical contact with the spectrometer then the sample is placed on a gold substrate, or a thin film of gold is evaporated onto the surface. As the ESCA experiment is being carried out on the sample material, there is a simultaneous monitoring of the Au_{4f} line. However, in depositing a metal film on the surface there is a tendency for the formation of metallic islands on the sample leading to differential charging of the surface. Another external standard used for energy referencing is the C_{1s} peak due to the contamination of hydrocarbons from the vacuum system. However, the buildup of a carbon layer on the surface from the vacuum system may take considerably longer time than the ESCA experiment allows due to low sticking coefficients of most organic polymers. Ideally, an external standard used to reference the energy scale of the spectrometer should have a well defined binding energy and not interact with the surface.

Another method of getting around surface charging problems of insulators is through the use of an internal standard. Internal standards, such as gold and indium may be implanted in the material before

analysis. Again, though, if the standard is a metal the problem of differential charging occurs because of the formation of isolated spots where the metal is located. Also, implanting a standard is likely to reorganize the chemical bonding of the sample in such a way that the chemical shifts obtained from the sample are not characteristic of the true chemical environment of the sample.

A third approach to the charging problem is through the neutralization of the surface charging by electron flooding. In this method a diffuse beam of electrons is washed across the surface while the ESCA experiment is being preformed. This method is detrimental to the analysis of the surface because of the damage caused by the flooding electron beam itself. Also, the determination of whether the sample is in electrical equilibrium is almost arbitrary.

Perhaps the best means of correcting for surface charging is a combination of one or more of these methods. However, some experimentalists believe that the problem of surface charging is inherent and cannot be overcome. The most noted of these is D. T. Clark at Durham, England[6]. He believes that surface charging is characteristic of the insulator being studied, but he has not yet presented a successful method of determining the charging characteristics of insulators.

Another difficulty in the interpretation of photoelectron peaks is caused by the surface sensitivity of electrons being emitted from the material. This problem can be directly related to the mean free path of electrons in the material. Because the depth at which an x-ray can cause ionization is much larger than the inelastic collision mean free path of an electron in the material, photoelectrons generated

at a distance in the material greater than this escape depth go
through multiple inelastic collisions. Consequently, these electrons
no longer have energies characteristic of the element and contribute
to an increase in the background count. The electron mean free path
is an important characteristic in quantitative and depth profiling
analysis.

The electron mean free path in the sample matrix is extremely im-
portant in the quantitative analysis of the sample using first prin-
ciples. However, the mean free path or escape depth also serves as a
useful parameter in the investigation of surface states. If the angle
with which the exiting electron leaves the surface is decreased, the
sampling depth is decreased, and the sampling area is increased. Con-
sequently, the peak intensities of only those atoms close to the sur-
face will be increased and the peak intensities of atoms deeper in
the sample will be decreased. This effect is extremely important in
the study of organic polymers, used in high voltage spark gaps, be-
cause the escape depth is on the order of 50-100 Å. Using grazing
angle incidence of the x-ray beam can effectively decrease the sam-
pling depth. Analysis of the thickness of thin films on metal surfaces
is also enhanced by this technique.

Another method of depth profiling via ESCA is through the use of
sputtering. Sputtering is the removal of layers of a sample by using
either an ion beam or an electron beam. In this process an ion or
electron beam is focused on the surface of the material during analy-
sis by ESCA. However, this process has two inherent difficulties.
First, selective sputtering of elements is an extremely complicated

problem. Because the cross-section for the removal of atoms from the surface is different for each element, the ion beam causes the removal of surface atoms at different rates (selective sputtering). Because the yields of secondary ions from a surface is sensitive to the surface state, the matrix, and the effects induced by the ion beam, a comparison of the ESCA peak intensities from a sputtered surface is not always a measure of the relative concentration of the atoms on the surface. Secondly, the process of sputtering significantly changes the chemical state of the material being analyzed. Consequently, depth profiling via ion or electron etching is not a very profitable technique because the information is not always representative of the surface in question.

Because the cross-section for ionization of all elements by x-rays is not the same, the sensitivity of ESCA for all elements is not the same. This poses another problem in the qualitative analysis of the ESCA spectrum. Wagner[7] has shown that there is a systematic variation of the sensitivity of an element to x-ray absorption throughout the periodic table. He has normalized the sensitivity of x-ray absorption to that of fluorine. Other work has subsequently been done to normalize the x-ray absorption cross-section to that of carbon. These sensitivity factors can be found in the literature and used to help make quantitative analysis more exact[8].

One last problem in the qualitative analysis of the ESCA spectrum is the presence of shake-up and shake-off lines. Even though shake-up and shake-off lines may help to identify surface structure in materials, they may also serve to obscure other peaks from the material.

However, because the satellite structure seen from a photoelectron peak is significantly different from that of a primary photoelectron peak this effect is usually minimal.

The largest single problem in quantitative analysis is reproducibility. Evidence seems to show that the intensity of photoelectron emission by an element is strongly dependent upon the screening of electrons by atoms that are nearest neighbors. Also, the intensities of lines depend upon the cross-section for photoionizing a given element in a given matrix. Because of these two phenomena, quantitative analysis via ESCA is mostly through the use of suitably prepared standard samples. However, this report will attempt to give a method of quantitatively analyzing materials through first principles calculations[9]. The intensity of a photoelectron peak from an elemental species in a material is given by,

$$I_s(E_i,x) = I(h\nu) \cdot \sigma_i(h\nu,\theta,x) \cdot \lambda s(E_i) \cdot N_i \cdot G \cdot H \qquad (2)$$

$$I_s(E_i,x) = A\eta f \sigma \phi y T \lambda C, \qquad (3)$$

where

f = x-ray photon flux in photons/cm^2s,

A = sample area from which photoelectrons are detected,

η = number of atoms of the element/cm^3,

λ = cross-section per atom for photoionization of the particular level,

σ = mean free path for the photoelectron in the sample medium,

T = inherent efficiency of dete··· n by the spectrometer of electrons originating from the sample,

y = fraction of photoelectric transitions from the given level that result in an ion in the ground state and a photoelectron of the ap-

propriate kinetic energy.

$\phi=$ angular correction factor,

$C=$ fractional efficiency of emergence through the surface.

Rearranging Eq. (3) yields:

$$n = \frac{I}{Af\sigma\phi y T\lambda C} = \frac{I}{S} , \qquad (4)$$

with S being a constant for a given element in a given matrix with a

given spectrometer. Therefore, for two different elements in the same

material,

$$\frac{n_1}{n_2} = \frac{I_1/S_1}{I_2/S_2} \qquad (5)$$

Consequently, if the sensitivity factors S_1 and S_2 are known for each

element then a relative measure of the number of atoms of each element

can be obtained.

There are many problems that can occur with this first principles

technique:

1) The flux, f, can vary with time in measuring the intensities

    of the two peaks. The reason for this is that in the ESCA

    experiment, first a broad spectrum of the sample is taken

    and then the region around each peak is analyzed separately

    to give better resolution. However, this problem is minimal

    with good x-ray sources.

2) If the lines differ significantly in kinetic energy, the

    mean free path ratio can vary among chemical states. How-

    ever, it has been shown experimentally that the mean free

    path of an electron is approximately given by $\lambda = aE/(\ln E - b)$

where a and b are constants that have been tabulated for many elements in many different materials. Figure 2-3[3] shows the relationship between the mean free path and the energy of the electron.

3) The photoelectron cross-section can vary slightly with the chemical state. However, tabulated values of cross-sections of different elements for different matrices can be found in A.W. Czanderna's book, Methods of Surface Analysis.

4) The probability of multielectron processes, (shake-up and shake-off) vary from atom to atom in various compounds. This is especially serious in aromatic compounds compared to acraphylic compounds.

5) The baseline of the spectrum is extremely important in determining the background count for each peak. The baseline of each peak must be chosen so that errors in the ratio of I_1/I_2 are minimal. The use of computers helps alleviate this problem, as well as the problem of peak deconvolution, where two or more peaks have similar energies.

Because of the difficulties present in first principles calculations of the number of atoms in a material, the best and most widely used method of quantitative analysis is the use of suitably prepared standards. Standards for quantitative analysis must be prepared and handled in a manner similar to the material to be analyzed. This poses numerous problems because standards must be prepared for every element in every matrix before the use of standards can be efficient.

Quantative analysis with ESCA is at most semi-quantative and at
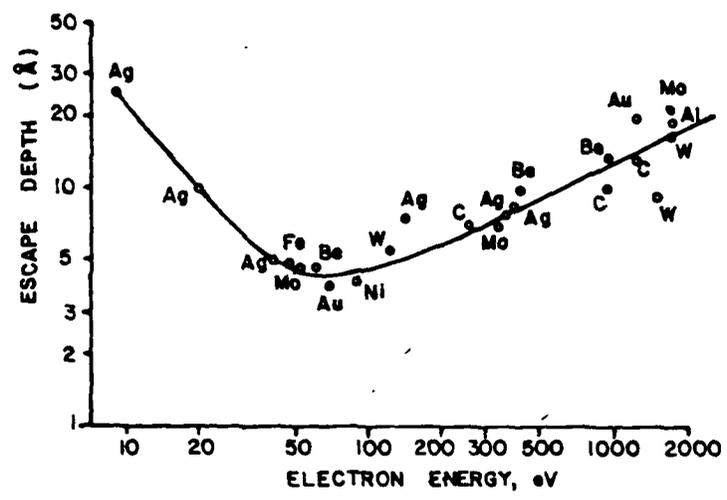
Figure 2-3 Electron escape depth vs. kinetic energy in metals. (ref. 3).

least a good guess. There is one good point about quantitative analysis via ESCA, the intensity of different elemental peaks, when properly corrected for their x-ray absorption cross-sections, can give useful information about the stochiometry of the material. Since stochiometry is generally the information most wanted when doing surface analysis, ESCA is a valuable tool. For example, it has been shown that various organic polymers when subjected to both direct and radiated energy transfer from a plasma exhibit large changes in the concentrations of various elements in the sample[10].

In these experiments, samples were placed in a chamber and irradiated in plasmas of nitrogen and argon for various lengths of time. The analysis of the sample was performed both before and after irradiation. The samples all showed significant increases in the amount of nitrogen present on the sample after irradiation (with both ions from the plasma and ultraviolet radiation), which was attributed to the formation of free radicals on the surface. These free radicals accepted nitrogen atoms from the plasma and/or absorbed species in the plasma chamber. The conclusion was that apparently nitrogen acts as a scavenger of free radicals. This could make the use of ESCA extremely valuable in the investigation of common insulators used in high voltage spark gaps.

Perhaps the most important aspect of ESCA as an analytical technique is the information derived from shifts in the binding energies of different elements because of the chemical environment. These shifts in binding energy can be used to identify structural features in the sample if these shifts can be correlated to some known effect

or if a qualitative theoretical method can be employed.

The origin of these chemical shifts results from changes in the chemical environment of the element being analyzed. Core orbitals are localized on atoms, their energies are sensitive to the electronic environment because of the screening effects of the valence electrons on the core electrons during ionization. If some of the valence electrons are removed by chemical bonding, the core level potential is more attractive and the binding energy is increased. This effect is especially pronounced in highly electronegative elements, such as fluorine. Many theoretical attempts to calculate shifts in binding energies have been published[11]. One such attempt has been to use a modified application of Pauling electronegativity calculations.

In these calculations the binding energy is given by

$$E_b = K_A q_A + \sum q_b/r_{ab} + E_R^o , \tag{6}$$

where

E_R^o = reference level,

$K_A q_A$ = contribution from net normal charge on atom,

$\sum q_b/r_{ab}$ = field contribution from nearby atoms.

The charge density is calculated through the use of the Pauling electronegativity equation,

$$q_i = Q_i + \sum_{i \neq j} nI_{ij} \tag{7}$$

where,

Q_i = normal charge on atom i,

n = number of bonds in which it is involved,

I_{ij} = partial ionic character of the bond between atoms i and j.

The partial ionic character, I_{ij}, can be expressed as

$$I_{ij} = 1-e^{-0.25(X_i-X_j)^2} \tag{8}$$

where X_i and X_j are the Pauling electronegativity values of i and j. Therefore it is possible through this charge potential model to calculate the binding energy of a given electron, assuming the constant K_A is known and a matrix of the material is assumed.

Another theoretical method for calculating changes in binding energies is to correlate changes in electronegativity with the changes in binding energy. Here $\Delta E_b = K\Delta q$ where ΔE_b represents the change in binding energy and Δq represents the change in electronegativity. This approach was suggested by the apparent linear change in binding energy related to electronegativity. Consequently, for a given element the constant K may be calculated and used to predict the change in binding energy for that element assuming a change in the electronegativity. Figure 2-4[4] shows the relationship between the change in binding energy of carbon for different electronegative elements and the electronegativity of the molecule.

The use of shifts in binding energies to interpret chemical structure is best shown by giving pictorial examples. Figure 2-5[1] and Fig. 2-6[1] give some idea of the chemical information available. In these two figures the carbon binding energy is given for carbon bound to different atoms. From these figures it is easily seen that ESCA can give well resolved information about the chemical environment of an atom. Clark, et. al.[1] have tabulated many of their results for changes in the binding energy of carbon and oxygen due to bonding of these elements with fluorine compounds. Therefore the identification of the chemical environment which effects the binding energy of carbon
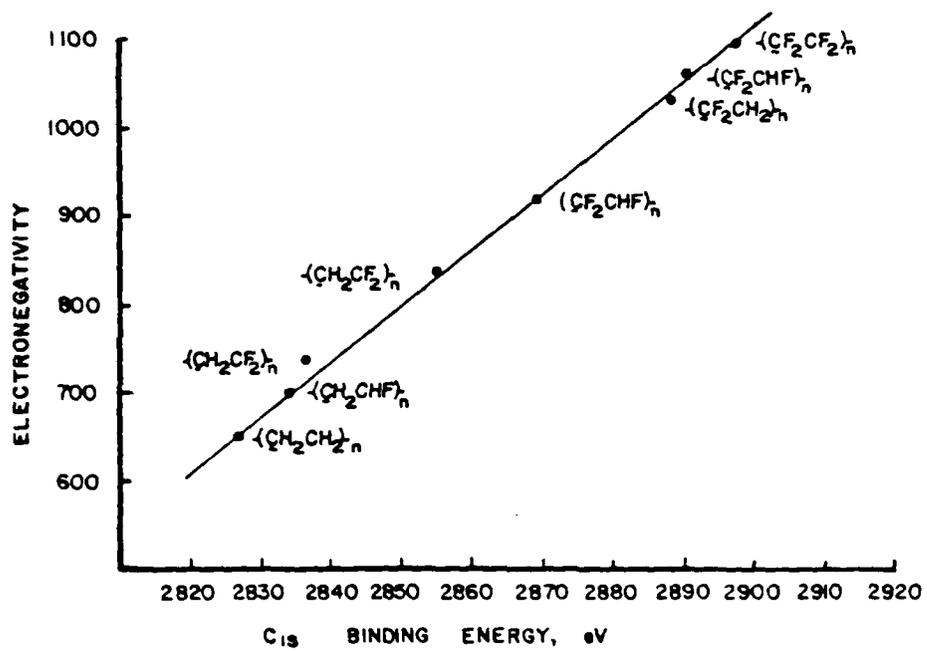
Figure 2-4 Relationship between the C_{1s} binding energy electro-
negativity of the compound. (ref. 4).

$$\left[CH_2 - CH_2 \right]_n$$

$$\left[CFH - CH_2 \right]_n$$

293 291 289 287 285 283

BINDING ENERGY (e.V.)
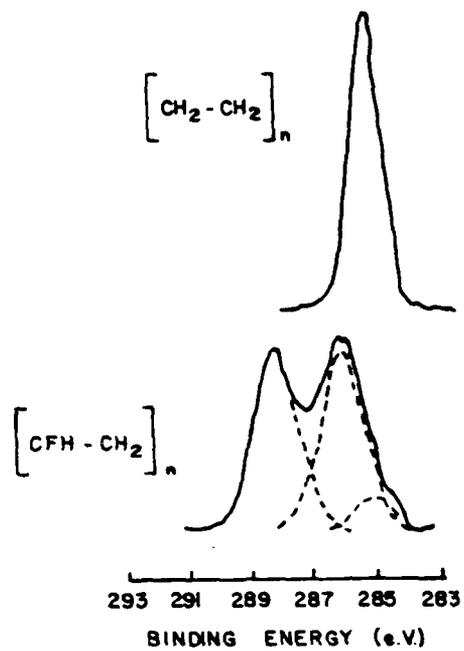
Figure 2-5 C$_{1s}$ levels of polyethylene and polyvinylfluoride. (ref. 1).

$$\left[CFH - CFH \right]_n$$

$$\left[CF_2 - CH_2 \right]_n$$

293 291 289 287 285
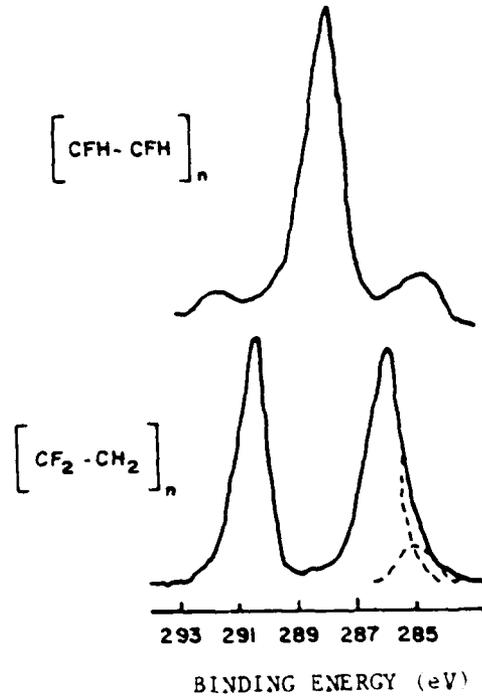
BINDING ENERGY (eV)

Figure 2-6 C$_{1s}$ levels of polyvinylenefluoride and poly-vinylidenefluorine. (ref. 1).

and oxygen atoms is made somewhat easier. Also, Phi Electronics have

published a Handbook of X-Ray Photoelectron Spectroscopy in which the

binding energy of all elements is given as well as the binding energy

of these elements with different chemical environments.

ESCA, because of its relative sensitivity and ease of analysis

as well as the amount of chemical information available from a single

spectrum makes it the most versatile analytical tool available today

for the analysis of insulators. Clark[1,2,6], et. al. have shown in

a series of papers on ESCA that using ESCA it is possible to study in

some detail the important chemical, physical, mechanical, and electri-

cal properties of polymers. Since ESCA gives first hand information

about the changes that occur on or near the surfaces of polymers due

to the plasma irradiation, and since ESCA gives well resolved infor-

mation about the chemical environment, as seen in fig. 2-5 and 2-6,

it is apparent that the use of ESCA for the investigation of the in-

sulators used in high voltage sparks gaps is essential.

LIST OF REFERENCES

1. D. T. Clark and W. J. Feast, "Applications of Electron Spectroscopy for Chemical Applications (ESCA) to Studies of Structure and Bonding in Polymeric Systems," *Journal of Macromolecular Science-Review Macromolecular Chemistry*, C12(2), 191 (1975).

2. D. T. Clark, "ESCA Applied to Polymers," *Advances in Polymer Science*, 24, 126 (1977).

3. P. F. Kane and G. B. Larrabee, ed., *Characterization of Solid Surfaces*, (Plenum Press, New York, 1974), 307.

4. A. W. Czanderna, ed., *Methods of Surface Analysis*, (Elsevier Scientific Publishing Company, New York, 1979), 103.

5. D. M. Hercules, "Electron Spectroscopy. I, X-Ray Photoexcitation," *Analytical Chemistry*, 44, 106, (1972).

6. D. T. Clark, A. Dilks, and H. R. Thomas, "ESCA Applied to Polymers. XXI. Investigation of Sample Charging Phenomena," *Journal of Polymer Science: Polymer Chemistry Edition*, 16, 1461, (1978).

7. C. D. Wagner, "Sensitivity of Detection of the Elements by Photoelectron Spectrometry," *Analytical Chemistry*, 44, 1050, (1972).

8. A. J. Bearden, "X-Ray Photoeffect Cross Section in Low and Middle Z Absorbers for the Energy Range 852 eV-40 keV," *Journal of Applied Physics*, 37, 1681, (1966).

9. C. J. Powell, "The Physical Basis for Quantitative Surface Analysis by Auger Electron Spectroscopy and X-Ray Photoelectron Spectroscopy," *Quantitative Surface Analysis of Materials*, ASTM STP, 643, 5, (1978).

10. H. Yasuda, H. C. Marsh, S. Brandt, and C. N. Reilley, "ESCA Study of Polymer Surfaces Treated by Plasma," *Journal of Polymer Science : Polymer Chemistry Edition*, 15, 991, (1977).

11. T. D. Thomas, "ESCA Binding Energies," *Journal of the American Chemical Society*, 92, 4184, (1970).

Chapter 3

Auger Electron Spectroscopy (AES)

Auger Electron Spectroscopy is one of the most widely used techniques for the study of the chemical composition of surfaces[1,2,3]. If the inner shell of an atom is ionized, by a beam of electrons, the atom has a finite probability of returning to a less energetic state either by the emission of a characteristic x-ray or through a radiationless process in which an outer shell electron is ejected with energy characteristic of the atom. These electrons are known as Auger electrons, and the energy analysis of these electrons constitutes the study of surfaces by Auger Electron Spectroscopy.

AES (the common acronym for Auger Electron Spectroscopy) is attractive as a surface analysis technique for several reasons. First, the depth from which Auger electrons can be detected is approximately 10-50 $\overset{\circ}{A}$. Consequently, AES is capable of measuring only the first few atomic layers of a material, allowing for the identification of surface contaminants. Second, the relative sensitivity for the emission of Auger electrons from atom to atom varies by less than a factor of 10, except for H and H_e which cannot be observed. Third, the AES data acquisition time is short compared to other techniques[4].

However, AES has a few unattractive features as well[5]. The depth from which the Auger electron is generated depends on the energy of the electron and therefore varies from element to element. Calibration of the escape depth as a function of energy has been published and is shown in Fig. 2-3. These calibration data provide a convenient means of determining the approximate depth from which an Auger electron has been emitted. Also, the electron bombardment required

28

for AES analysis, typically 5-25 keV electrons, can affect the chemical environment of the sample. A third problem is that in multielement materials different atomic Auger electron peaks may often have similar energies. However, usually there is more than one observable peak per element which helps identify different elements present in the example. Usually the shape of the peaks is also different from level to level which aids in the identification of different elemental peaks.

When the incident electron ionizes the core level, the vacancy is immediately filled by another electron. The energy from this transition is then released in the form of an Auger electron. Consider, for example, the ionization of an electron in the K shell where the vacancy is then filled by an electron from an L shell. The energy of the transition is $E_K - E_L$. This energy is then given to another electron or a characteristic x-ray depending upon the probability for each event (see Fig. 3-1)[6]. The total energy of the Auger electron is dependent upon the energies of the three shells involved in the process as well as the work function of the material being examined. Fig. 3-2[7] shows the relation of the energy of the shells to that of the Auger electron.

From this figure,

$$E(Z) = E_K(Z) - E_{L_1}(Z) - E_{L_{2,3}}(Z+\Delta) - \Phi$$

where

$E(Z)$ = energy of Auger electron,

$E_K(Z)$ = ionization energy of an electron in the K shell,

$E_{L_1}(Z)$ = ionization energy of an electron in the L shell,

$E_{L_{2,3}}(Z+\Delta)$ = ionization energy of an electron in the $L_{2,3}$ shell
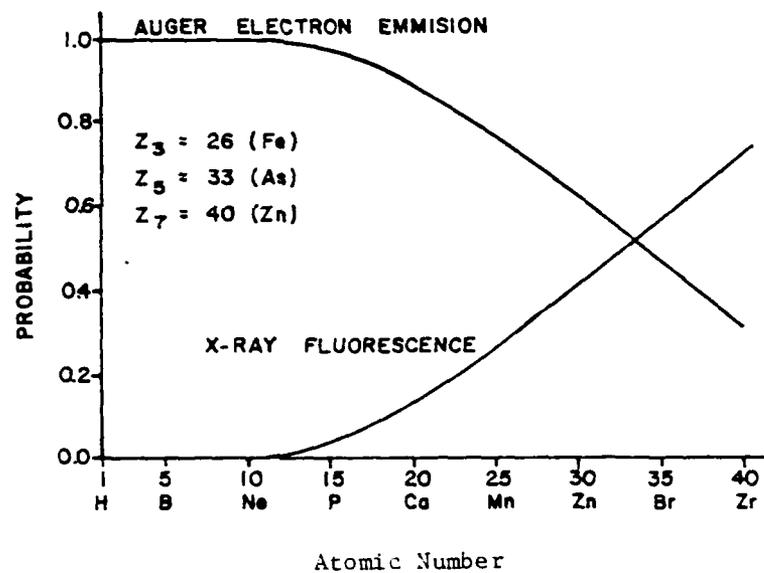
Figure 3-1 Probability of Auger electron emission and x-ray
fluorescence as a function of atomic number. (ref. 6).
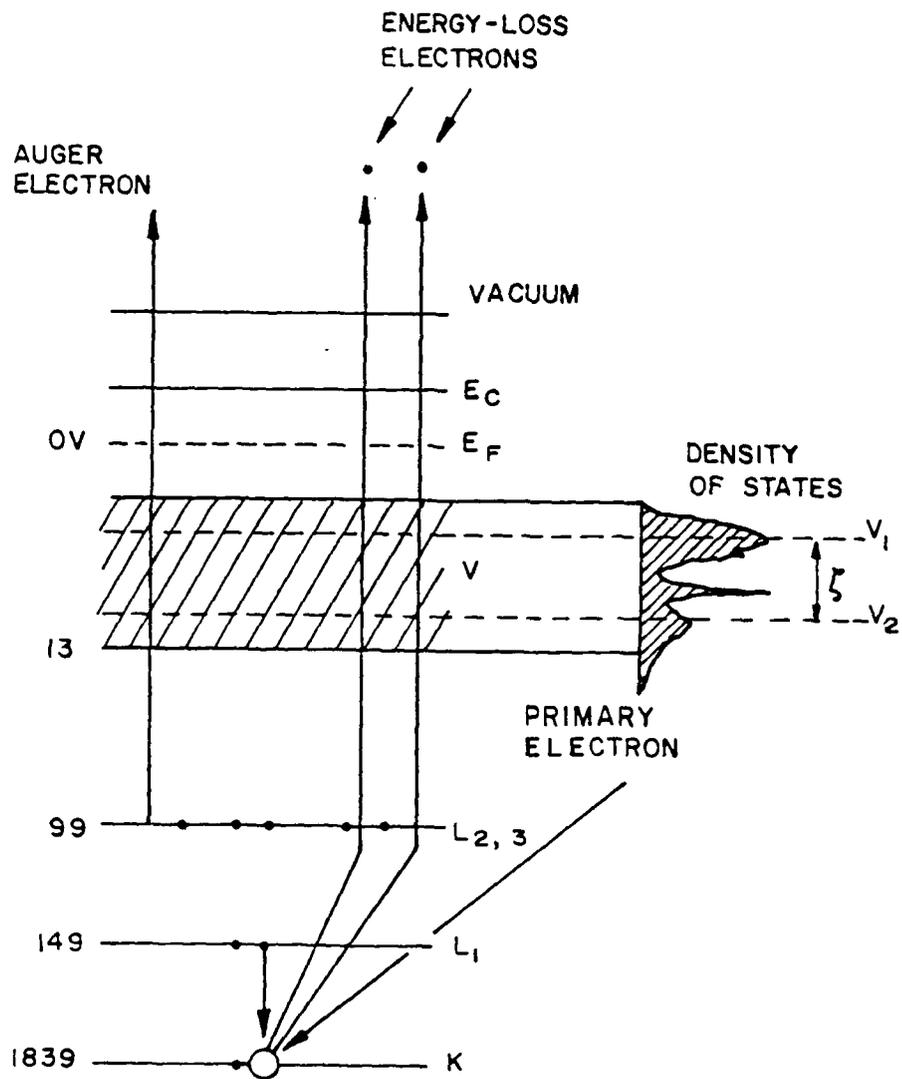
Figure 3-2 The singly ionized Si atom. The electronic energy levels
        are listed on the left (in eV) with the zero of energy
        at the Fermi level E_f: E_c is the bottom of the conduc-
        tion band. The x-ray nomenclature is given on the right,
        and the density of states has been drawn into the valence
        band. A $K_{L_1 L_{2,3}}$ Auger process is depicted, after primary
        electron ionization. (ref. 7).

with an extra amount of energy needed to overcome
the extra positive charge of the atom. Typical
values of Δ are usually between 1/2 and 3/2,

ϕ = work function of the material.

Due to the differences in work functions of the material and the spec-
trometer there is an additional term in the expression for the energy
of the Auger electron. The additional term is $-(\phi_A-\phi)$ where ϕ_A is
the work function of the spectrometer. Consequently, the energy of
an Auger electron can be approximated for any Auger event involving
three levels, WXY, as $E_{WXY}(Z)=E_W(Z)-E_X(Z)-E_Y(Z+\Delta)-\phi_A$.

First principles calculations of the Auger energies have been at-
tempted. However, these approaches suffer from a difficulty in relat-
ing the coupling schemes that govern the transitions from singly ion-
ized to doubly ionized states of atoms. Therefore, a first principles
calculation of the Auger energies is extremely complicated and another
method of qualitative analysis is employed. For a qualitative analy-
sis of the Auger electron peak energies a chart of the most prominent
AES lines can be found in the Handbook of Auger Electron Spectroscopy[8]
The energy of all electrons ejected from the material is ana-
lyzed. Because Auger electrons are superimposed on a background of
backscattered primary electrons and secondary electrons ejected as
a result of the primary electron beam bombardment, the derivative of
the total number of electrons with respect to the energy is measured.
This allows the Auger electron energies to be relatively more pro-
nounced on the spectrum than the constant background. A typical spec-
trum obtained by AES is shown in Fig. 3-3[3], which compares the sig-
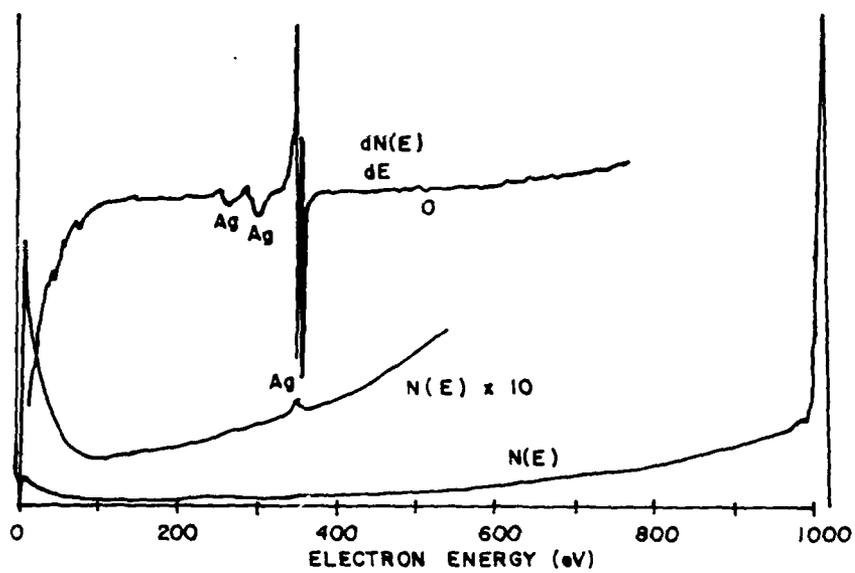
Figure 3-3 Energy distribution N(E) and dN/dE for a silver
target with primary beam of electrons at 1000 eV
(ref. 3).

nals from the differentiated and undifferentiated spectra. The
energy of the peak is the Auger energy and using the chart of prom-
inent Auger electron energies it is possible to determine which
element is responsible for the peak. However, if two or more ele-
ments with similar Auger electron energies are present within the ana-
lysis depth of AES they will be superimposed on the spectrum.

The escape depth, or mean free path for inelastic collisions,
is the largest factor contributing to the high surface sensitivity of
AES[2]. Auger electrons may lose energy through plasmon losses, core
excitations, or interband transitions. Plasmon losses occur when an
Auger electron loses discrete amounts of energy to the excitation of
valence electrons. Core excitation losses occur when Auger electrons
serve to excite atoms to emit characteristic Auger electrons. Inter-
band transition losses occur when Auger electrons collide inelastical-
ly with atomic electrons in either valence or core levels. However,
Auger electrons which lose their energy through these processes no
longer contribute to the Auger peak but instead contribute to the
background. The escape depth is determined experimentally by deposi-
ting a thin film of known composition on metallic substrates while
observing the decrease in intensity of the Auger peaks from the sub-
strate. Since the escape depth is an extremely important parameter
in the quantitative analysis of materials it is important to know
the escape depth as a function of energy and matrix. Experimental
values of the escape depth are shown in Fig. 2-3.

Quantitative analysis of the Auger peak can be achieved by
three different methods. A first principles calculation of the Auger

current is given by the equation:

$$I_s(E_i, WXY) = I(E_o)r_i(E_o, E_w)r_{s,i}(E_o)\sigma_i(WXY)N_i\lambda_s(E_i) \cdot G \cdot H$$

where

$I_s(E_i, WXY)$ = current due to Auger transition WXY for element i in matrix S,

$I(E_o)$ = current incident upon sample at energy E_o,

$r_i(E_o, E_w)$ = ionization cross-section for level W of ith species,

$r_{s,i}(E_o)$ = backscatter correction for i^{th} species in matrix S,

$\sigma_i(WXY)$ = probability for Auger transition WXY,

N_i = density of atoms i,

$\lambda_s(E_i)$ = inelastic mean-free path for electrons of energy E_i in matrix S,

G = constant for source geometry,

H = constant for analyzer geometry.

First principles calculations of the intensities of Auger peaks are extremely complex due to the interdependence of the factors. For example, the incident current on the sample is dependent upon the depth in the sample, diffraction effects, incident angle, and multiple ionizations by both the incident beam and also the Auger electrons which go through inelastic collisions. Calculations of the escape depth involve complicated functions of the material matrix and the energy of the Auger electron. An approximate expression for the escape depth as a function of energy is $\lambda = aE/(\ln E - b)$ where "a" and "b" are constants that have been tabulated for many different elements and matrices. The ionization cross-section for electron bombardment is another factor which creates difficulties in calculating Auger currents. The approx-

imate ionization cross-section is shown in Fig. 3-4[7]. However,

since the primary electrons cause the emission of secondary elec-

trons, some with sufficient energy to cause the emission of more

Auger electrons, a correction factor is necessary to get an accurate

value of the Auger current. Therefore, the back-scattering correc-

tion term must also be known before first principles calculations can

be accurate. Perhaps the most important factor to be considered in

first principles calculations is the probability of deexcitation of

the atom by the Auger event. The probability of x-ray emission[9],

the process competing with Auger electron emission, is given by:

$$\omega = (1 + AZ^{-4})^{-1}$$

where $a = 1.12 \times 10^6$ for K-electrons,

$$= 6.4 \times 10^7 \text{ for L-electrons,}$$

and is dependent upon the energy of the incident radiation, whether

it is electrons or photons,

Z = atomic number.

The probability of x-ray emission for 0-2 keV incident electrons is

approximately 0.032 for K-shell ionizations and 0.033 for L-shell ion-

izations which is negligible compared to Auger electron deexcitation.

Finally, the parameters G and H are dependent upon the spectrometer

being used and may be measured for the particular spectrometer assum-

ing that the same geometry is used each time a different sample is

to be analyzed.

Because of all these difficulties involved in the quantitative

analysis of the Auger spectrum by first principles, the best accuracy

that can be achieved is 40% of the concentration. Other methods of
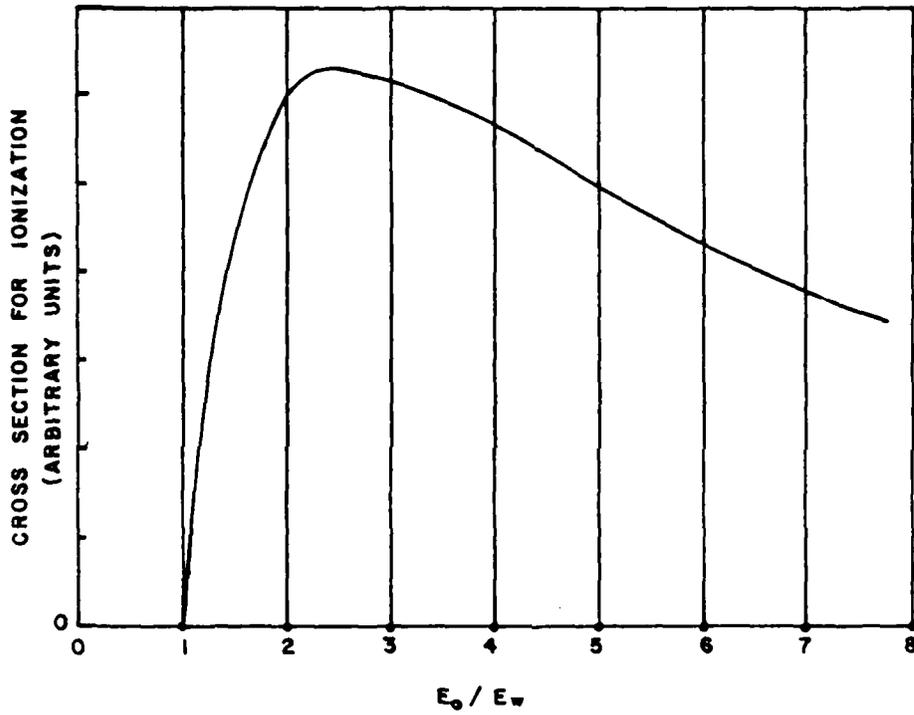
Figure 3-4 Ionization cross section vs. reduced energy E_0/E_w , where E_0 is the primary electron energy and E_w is the critical energy of ionization. (ref. 7).

quantitative analysis can be used for better accuracy. One such

method is to use suitably prepared standards. The Auger spectra of

the material to be analyzed is compared with the Auger spectra of a

standard with known concentration of the element of interest. The

test material and the standard must be measured and prepared under

identical conditions. If these conditions are met then the follow-

ing relationship for the concentration and intensities of the ele-

ment in the known and unknown samples is:

$$\frac{C_i \text{ unknown}}{C_i \text{ standard}} = \frac{I(E_i, WXY) \text{ unknown}}{I(E_i, WXY) \text{ standard}} .$$

One important advantage in using this method of quantitative analysis

is that ionization cross-sections and Auger yield data are not requir-

ed if the materials are analyzed under similar conditions. However,

if the concentration of the element in question is significantly dif-

ferent in the reference material, compared to the material to be anal-

yzed, it is necessary to make corrections for backscattering and es-

cape depth as a function of the matrix involved. Because of this dif-

ficulty this method lacks the ability to give an easy and rapid quan-

titative analysis.

Another approach to the quantitative analysis of Auger spectra is

to use elemental sensitivity factors. This method is less accurate be-

cause variations in the backscattering factor and escape depth are not

taken into account. If sensitivity factors can be assigned to each and

every element then the concentration of an element in a material may

be calculated using the expression

$$C_x = (I_x/S_x)/\Sigma(I_\chi/S_\chi),$$

where S_α is the relative sensitivity factor of element α. Because external standards are not needed and the geometry factors are the same for all elements this method has certain advantages over the other two methods.

Quantitative analysis by AES is at most 70% accurate by any of the above three methods. Consequently, if the only information desired from the material is the elemental concentration then AES is not the best available analysis technique to use.

Depth profiling with AES is possible with the use of ion etching. Simultaneous sputtering with an ion beam and analysis with an electron beam have the advantage that surface destruction is greatly reduced. In order to perform depth profiling an ion beam with an effective diameter greater than that of the electron beam is focused on the material. Simultaneous with the sputtering process the Auger current is measured at the center of the crater being formed. Ion bombardment of the sample has little effect on the Auger peaks because the cross-section for ionization of an atom by an ion beam is much smaller than by an electron beam.

The uniformity of the ion beam across the sampled area, the Auger electron escape depth, the sample inhomogeneity are all factors which affect the depth resolution of a simultaneous AES and ion etching depth profile. However, since the ion beam is much larger than the electron beam, nonuniformity of the ion beam is not a major factor in the depth resolution as long as the Auger current is taken from the center of the crater. Also, the effect of the Auger electron escape depth is not important if the matrix of the sample does not change

significantly as a function of the depth and if the Auger analysis
is done at normal incidence. Therefore, the only major factor that
inhibits depth profiling is sample inhomogeneity. For example, if
a thin film is present on a substrate the magnitude of the Auger
current may change considerably in moving from the film to the sub-
strate because of variation in sputtering yields. Also, there is a
definite probability that the ion beam will leave ions on or in the
surface to be analyzed.

Because the binding energies of core electrons can change with
changes in the chemical environment, chemical effects can be observed
in Auger spectra. This is especially the case for insulators where
valence electrons play an important role in bonding. Changes in the
chemical environment of an element are manifested as changes in the
shape of Auger lines, shifts in the expected Auger electron energies,
or changes in the relative intensity of an Auger line. Fig. 3-5[3]
shows the usual shape of an Auger line. However, if the chemical en-
vironment is changed the shape of these lines may change drastically.
The shape of the line is a consequence of the probability of a given
transition. From first principles calculations of the energy of an
Auger line using a particular coupling scheme, an idea of the number
of spikes to be expected can be obtained by claculating the probabili-
ty density of a transition from one state to another. If, however,
the chemical state of the material is changed then the wavefunctions
used to calculate the energy can also drastically change, causing a
change in the probability density of a particular transition. For an
example of peak shape changes because of valence level bonding changes,
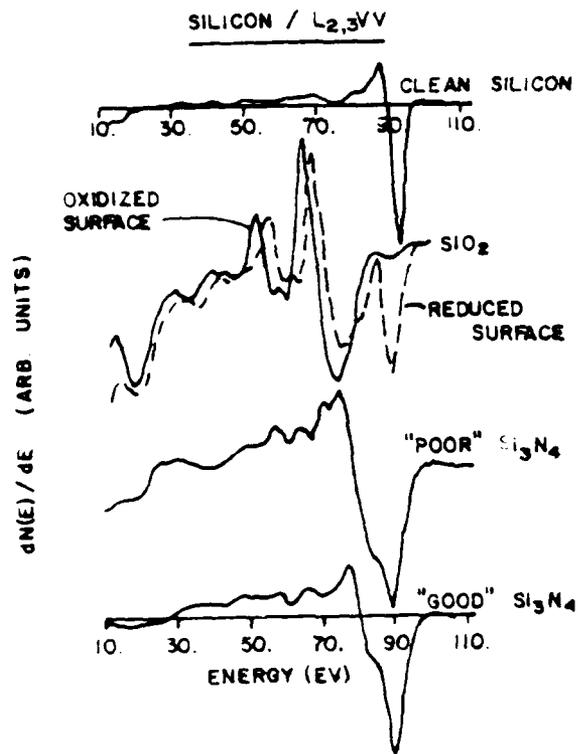
Figure 3-5 Changes in the shape of the Si Auger peak due to differences in chemical environment. (ref. 3).

refer to Fig. 3-5[3]. The change in relative intensities between
groups of Auger lines is another important consequence of changes
in chemical environment. Ejection of an Auger electron from a valence
level is affected a great deal more by the chemical environment than
the ejection of an Auger electron from a core level. This is because
the valence band bonding is weaker than the core level bonding and the
probability for the Auger event to occur is much greater in the valence
level. Therefore, the intensity of core level Auger lines and valence
level Auger lines is drastically different.

Another consequence of the chemical environment on the Auger
line is the shifts in energy that can occur. Shifts in Auger energy
lines are caused by structural rearrangements of valence bonds. When-
ever the electron density around an atom is decreased by the transfer
of electrons to another atom, the binding energies of the remaining e-
lectrons are increased. The transfer of electrons from one atom to ano-
ther is especially prevalent for electronegative atoms, such as fluorine.
The shifts that are measured are the result of the shifts in the three
energy levels that are involved in the Auger transitions, and consequent-
ly the shifts may be very small.

The principle problems in the measurement of changes in the Auger
energy lines are resolution and sensitivity as well as surface
charging of insulators. The resolution and sensitivity problems arise
because the Auger lines themselves are a few eV wide, and therefore it
is difficult to accurately measure changes of only a few eV. The sur-
face charging of insulators was discussed in the chapter on ESCA.

However, it appears that the problem of surface charging in AES is more complicated and harder to overcome. In AES, a surface with a secondary electron emission coefficient (a number representing the ratio of emitted secondary electrons to the incident electrons) less than one is driven towards a negative potential. In ESCA the surface is positively charged and can be compensated for by flooding the surface with low energy electrons. However, a negative surface charge cannot be overcome by electron flooding and positive ion flooding is of little help because the electron current densigy is usually orders of magnitude larger than the ion current density. Lowering the energy of the incident electron beam or using oblique electron incidence both increase the secondary electron emission, however in most polymer targets the yield of secondary electrons is still less than one. It is possible to use AES to analyze an insulator target with secondary electron emission coefficient equal to one because the surface is usually neither positively nor negatively charged.

AES is a very useful technique for the analysis of many different types of materials. It is especially well suited for the analysis of conductors since the problems of surface charging are avoided and because of the well-defined results published for many conductors. However, the use of AES to analyze the insulators used in high voltage spark gaps is probably of little value, due to the surface charging problems.

LIST OF REFERENCES

1. E. N. Sickafus, "Surface Characterization by Auger Electron Spectrometry," Journal of Vacuum Science Technology, 11, 299, (1974).

2. A. W. Czanderna, ed., Methods of Surface Analysis, (Elsevier Scientific Publishing Company, New York, 1979), 159.

3. R. E. Weber, "Auger Electron Spectroscopy for Thin Film Analysys," Research/Development, October, 22, (1972).

4. J. W. Coburn and E. Kay, "Surface Analysis Today," Research/Development, December, 37, (1972).

5. T. W. Haas, J. T. Grant, and G. J. Dooley III, "Some Problems in the Analysis of Auger Electron Spectra," Journal of Vacuum Science Technology, 7, 43, (1969).

6. P. F. Kane and G. B. Larrabee, ed., Characterization of Solid Surfaces (Plenum Press, New York, 1978), 310.

7. P. F. Kane and G. B. Larrabee, ed., Characterization of Solid Surfaces, (Plenum Press, New York, 1978), 509.

8. L. E. Davis, et. al., Handbook of Auger Electron Spectroscopy, (Physical Electronics Division, Perkin-Elmer Corporation, Eden Prairie, Minnesota, 1978).

9. H. E. Bishop and J. C. Riviere, "Estimates of the Efficiencies of Production and Detection of Electron-Excited Auger Emission," Journal of Applied Physics, 40, 1740, (1965).

10. T. W. Haas, J. T. Grant, and G. J. Dooley III, "Chemical Effects in Auger Electron Spectroscopy," Journal of Applied Physics, 43, 1853, (1972).

Chapter 4

Secondary Ion Mass Spectroscopy (SIMS)

Secondary Ion Mass Spectroscopy[1-4] involves the bombardment of
a surface with a probe beam of ions with energy between 1 and 20 keV.
This beam sputters or erodes the surface away a monolayer at a time.
As a result of the ion impact, atomic and molecular particles, elec-
trons, and photons are emitted from the surface. The atomic and mole-
cular particles may be either in a neutral or charged state. The par-
ticles can be in either excited or ground states. Mass analysis of
the charged particles, which consist of both positive and negative
ions, gives elemental and often structural information about the chem-
ical composition of the surface.

When an ion is incident upon a surface there are several possible
events that can occur[3]. Figure 4-1 shows three of the possible
events. One possible event is reflection of the incident ion due to a
collision with a surface atom. The most probable event is that the in-
cident ion will penetrate into the surface and dissipate its energy to
surrounding atoms through elastic and inelastic collisions, eventually
becoming implanted in the matrix of the material. Sputtering occurs
when the atoms or molecules on the surface obtain both enough energy
and the correct direction from the incident particles to escape from
the surface. There is also the possibility of ejection of a highly
energetic particle through direct transfer of energy from the inci-
dent ion to the surface particle. This process is called recoil sput-
ering. The mass analysis of these particles is the basis for SIMS,
the common acronym for Secondary Ion Mass Spectroscopy.
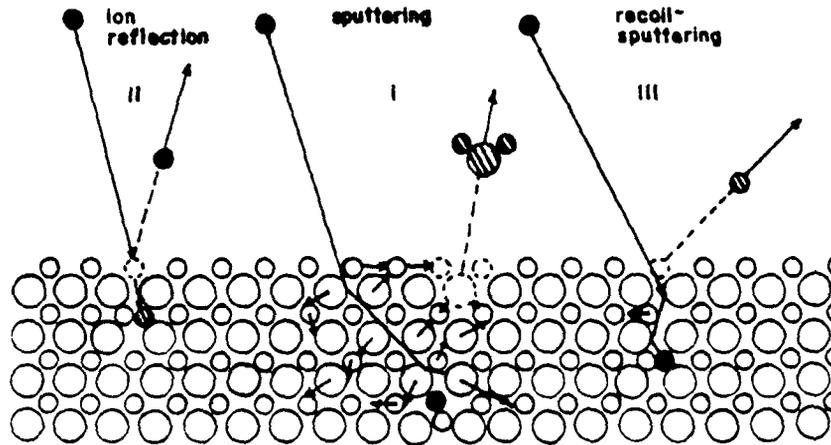
Figure 4-1 Interaction processes of an ion with a solid surface
resulting in the emission of heavy particles. (ref. 3).

The advantages of SIMS[5] over other techniques are that SIMS is able to detect all elements, including hydrogen. Also, SIMS can detect all isotopes present in a material. Another advantage of SIMS is that due to the use of conventional mass spectrometers the resolution of the SIMS spectrum is much greater than for most other techniques. The resolution of different surface analysis techniques is dependent upon the FWHM energy spread of the incident beam. Typically the FWHM for ESCA is .75-1.0 eV, for AES the FWHM is 1 eV, and for SIMS the FWHM is .1-.5 eV.

Even though SIMS is an important and useful technique for the identification of all elements on the surface, it suffers from several problems[6]. First, the incident ion beam is highly destructive. The incident ion beam causes the emission of surface species, the implantation of primary ions, changes of the lattice structure created by the emission of atomic and molecular species and by the implantation of the primary ions. Also, the incident ion beam causes changes in the chemical environment through the breaking of bonds and the formation of new bonds. To decide whether a sputtered atom or molecule leaves the surface as an ion or neutral is a complicated process involving the quantum mechanical analysis of ground and excited state interactions of the atom or molecule with the solid and surface electronic states. The number of processes that contribute to the secondary ion yield is large and varies from the ionization of the emitted species by Auger de-excitation to electron redistribution and ionization of surface compounds. Consequently, quantitative analysis is hindered because all of these processes must be

included for an accurate analysis. Finally, the depth resolution of the SIMS spectrum is affected by non-uniform sputter-etching. Non-uniform sputter-etching is caused by the large variations in the efficiency of emission of different ion species by the incident ion beam beam and also the nature of the matrix. The differences in efficiency of an ion emission for various elements is shown in Fig. 4-2[7]. The effects of the matrix on the sensitivity of ion emission can best be shown by the information in Table 4-1[8].

The escape depth for the analysis of sputtered species is dependent upon several parameters. The characteristics of the collision cascade have the strongest influence upon the escape depth. The collision cascade, a process by which particles are sputtered from the surface, is strongly dependent upon the incident ion beam energy and the masses of both the incident ion and target atoms, as shown by Fig. 4-3[7]. The escape depth is also influenced by the atomic binding energies. The escape depth is approximately 20 $\overset{o}{A}$ for most materials.

The positive or negative secondary ion yields[7], defined as S_A^-, is given by

$$S_A^\pm = \gamma_A^\pm \, C_A S \tag{1}$$

where

$$S_A^\pm = \frac{\text{number of ions of element A emitted}}{\text{number of incident primary ions}}$$

$$\gamma_A^\pm = \frac{\text{number of secondary ions, positive or negative, of element A}}{\text{number of neutral and charged particles}}$$

C_A = concentration of element A in the sample

S = total sputter atom yield (atom per incident ion).

The secondary ion yield, as defined above, is strongly influenced by the electronic and chemical properties of the surface. The two pos-
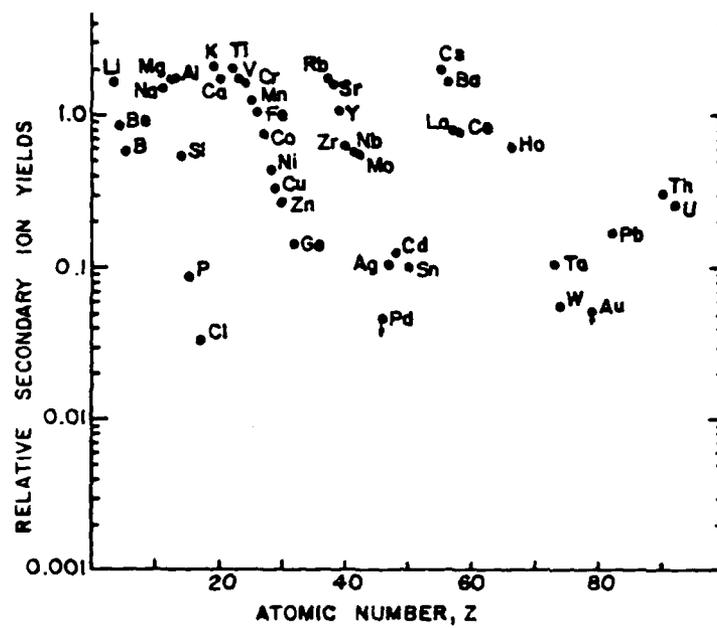
Figure 4-2 Relative secondary ion yields for a number of
elements in a refractory oxide matrix, for a
particular SIMS spectrometer. (ref. 7).

TABLE 4-1

Absolute secondary ion yields $S(Me^+)$ for clean and oxygen covered surfaces

Metal	$S(Me^+)$ Clean surfaces	$S(Me^+)$ Oxygen covered surfaces
Mg	0.01	0.9
Al	0.007	0.7
Ti	0.0013	0.4
V	0.001	0.3
Cr	0.0012	1.2
Mn	0.0006	0.3
Fe	0.0015	0.35
Ni	0.0006	0.045
Cu	0.0003	0.007
Sr	0.0002	0.16
Nb	0.0006	0.05
Mo	0.00065	0.4
Ba	0.0002	0.03
Ta	0.00007	0.02
W	0.00009	0.035
Si	0.0025	0.58
Ge	0.0044	0.02

(see references 8).
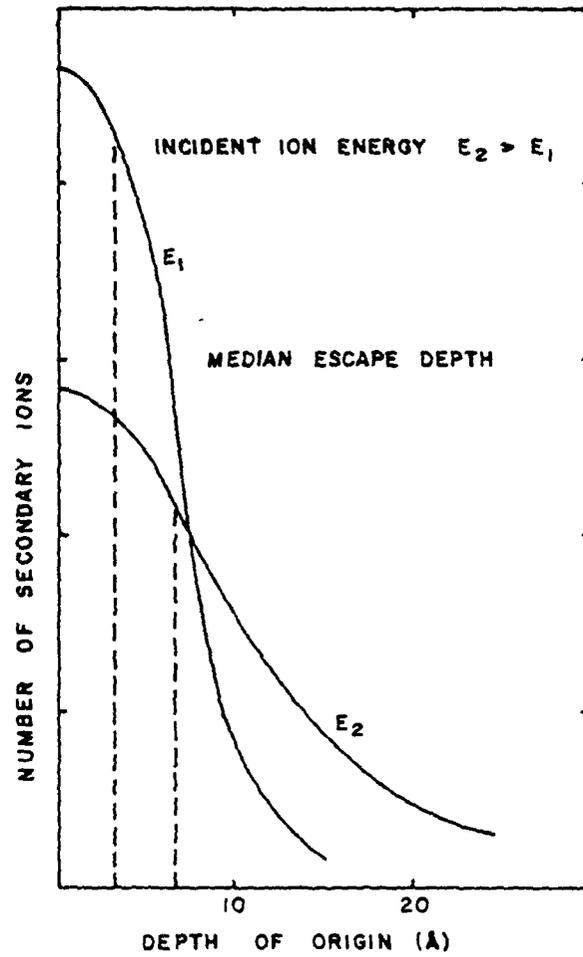
Figure 4-3 Hypothetical secondary ion depth-of-origin
for incident energies E_1 and E_2. (ref. 7).

sible means of secondary ion production are kinetic ionization and

chemical ionization. Kinetic ionization occurs outside the sample

surface through de-excitation of an excited neutral by an Auger elec-

tron ejection. Kinetic ionization is the predominant ionization proc-

ess for conductors because ions which are produced within the matrix

of the material are neutralized by free electrons. Chemical ioniza-

tion occurs because of the presence of chemically reactive species in

or on the surface which reduce the number of free electrons available

for neutralization of ions. The most chemically reactive species are

oxygen for the enhancement of positively charged secondary ions and

cesium for the enhancement of negatively charged secondary ions.

Since these two processes dominate in the production of secondary ions

and since they are both sensitive to the chemical variations in the

sample surface, the secondary ion yield may change because of chemical

variations and not necessarily because of concentration changes.

The ion current measured by the SIMS spectrometer is given by

$$i_A^{\pm} = \eta_A \, S_A^{\pm} \, I_P \tag{2}$$

where $i_A^{\pm}$ = secondary ion current,

η_A = ion collection efficiency of the particular SIMS spectrome-
ter,

I_p = total primary ion current incident on the sample.

The ion collection efficiency can be considered a constant, indepen-

dent of the sample, if the secondary ion energy distributions of dif-

ferent peaks are similar. The total ion current is as given above

for a monoisotopic element. If, however, the element in question has

more than one abundant isotope present in the sample an additional

factor must be considered. This additional factor is f_a, which is

the isotopic abundance for isotope a of element A. Therefore, the

ion current for a given isotopic component of a multi-isotope element

is $f_a i_A^{\pm}$. The primary ion current is dependent upon the primary ion

current density, D_p, and the diameter of the beam, d. The primary

ion current can be written as

$$I_p = \tfrac{1}{4}\pi D_p d^2 \tag{3}$$

for a uniform circular spot. Some typical values of the parameters

which determine the secondary ion current are:

$\gamma_A = 10^{-5}-10^{-1}$, S=1-10, A=$10^{-5}-10^{-2}$, D_p=$10^{-6}-10^{-2}$ mA/cm^{-2},

and d=$10^{-4}-10^{-1}$ cm, which when used in Eq. 2) and 3) give $i_A^{\pm} \approx .5$ mA

for a concentration of 1 mole.

Many models[1-2] have been published to attempt a calculation of

the absolute and relative secondary ionization probabilities for ele-

ments in different matrices. However, most of these theoretical argu-

ments do not sufficiently describe both the emission of negative and

positive secondary ions. Consequently, quantitative analysis by SIMS

is dependent upon trial and error calculations. The secondary ion

yields are mostly obtained from tables and graphs[8] which give the

relative yields of elements for a given matrix and incident ion ener-

gy. Another serious problem in quantitative analysis with SIMS is

the emission of secondary ions with a net charge greater than one be-

cause these ions sometimes interfere with other spectral peaks.

For a successful quantitative analysis by SIMS the spectrometer

operating parameters, such as primary ion species, energy and current,

sample environment, and detector efficiency must be standardized. Af-

ter the operating procedures have been standardized it should be possible to use relative sensitivity factors derived from suitably prepared reference standards to give quantitative analysis with SIMS. The sensitivity factor must be normalized for matrix effects. Combining the previous equations to obtain the ratio of the element of interest to some reference element gives the following expression:

$$\frac{i_A^{\pm} C_A^{-1}}{i_{ref}^{\pm} C_{ref}^{-1}} = \frac{\gamma_A^{\pm}}{\gamma_{ref}^{\pm}} = \delta_A \tag{4}$$

where $i_A^{\pm}$ and $i_{ref}^{\pm}$ are the intensities of the element in the matrix sample and of the reference element in a similar matrix. C_A and C_{ref} are the concentrations of the element in the matrix and of the reference element. $\gamma_A^{\pm}$ and $\gamma_{ref}^{\pm}$ are the ratios of the number of secondary ions produced to the total number of atoms sputtered. The relative elemental sensitivity factor δ_A can be used to relate the concentration of the element of interest to the intensity by

$$\left(\frac{i_A^{\pm}}{i_{ref}^{\pm}} \right) \delta_A^{-1} = \frac{C_A}{C_{ref}} \tag{5}$$

The problems with this method of quantitative analysis are that the sensitivity factors are valid only for matrices similar to those from which the factors were derived, the accuracy of the sensitivity factors depends upon the quality and nature of the standards, and the sensitivity factors are only valid for the particular spectrometer and operating conditions employed. For these reasons quantitative analysis with SIMS by the use of standards is extremely complex and the precision that can be expected is no greater than 50% under the best of of conditions.

For a better quantitative analysis a parameter, δ_s, should be de-

fined and standardized. This ε_s is a parameter that characterizes the electronic properties of the secondary ion-emitting surface. The relative sensitivity factors exhibit a dependence on ε_s as shown in Fig. 4-4[7]. Therefore ε_s can be defined as $\varepsilon_s = k(\delta_1/\delta_2)$ where k is an arbitrary constant and δ_1 and δ_2 are the relative sensitivity factors. Once the value of ε_s has been determined for a given matrix it is possible with reasonable accuracy to measure the relative sensitivity factors of the secondary ions from the surface and consequently the concentration of the element.

The parameter ε_s can best be derived from the ratio of multiplicharged species to singly charged species or from the ratio of molecular species to atomic species. Once this parameter has been standardized and its measurement has been standardized, quantitative analysis will become much more precise. At present, though, no reasonable approach to quantitative analysis of spectra from SIMS exists and until one is devised or until secondary ion yields of an element in any given matrix are standardized the use of SIMS as a quantitative instrument is limited.

The single most important advantage of SIMS over other techniques is its ability to detect all elements, including hydrogen. The detection sensitivity for an element is directly affected by the chemical composition of the material. In addition, the primary ion species and primary current that reach the sample, the solid acceptance angle and secondary ion transmission efficiency of the analyzer, and the general background of the spectrum are all dependent upon the geometry of the spectrometer. The chemical composition of the sample ma-
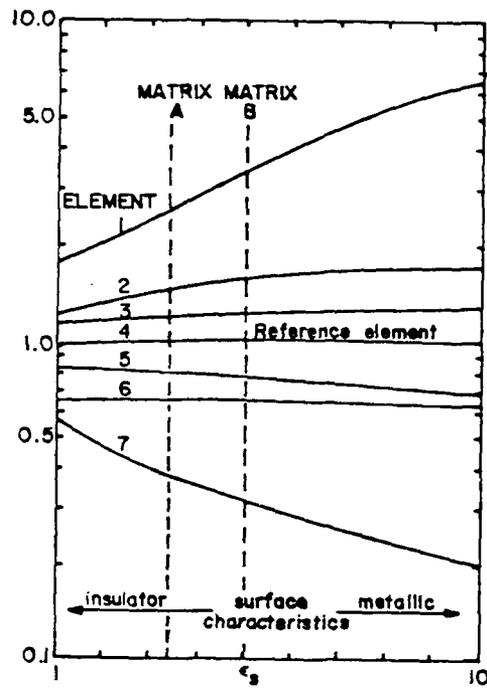
Figure 4-4 The dependence of the relative elemental
sensitivity factor on the character of the
sample surface. (ref. 7).

trix has a most important effect upon the secondary ion yield through
differences in the electronic properties of the materials. Also, the
matrix can affect the spectrum by the emission of molecular and multi-
ply charged particles which interfere with particular mass points of
interest. The differences in the secondary ion yield caused by ma-
trix effects has already been discussed in conjunction with the poss-
ible secondary ion production events. The emission of unwanted mole-
cular species and multiply charged species can be controlled by ei-
ther analyzing only those secondary ions with high initial energy or
by using a mass/charge analyzer with a resolution $M/\Delta M$ greater than
3000. Fig. 4-5[7] shows the relative secondary ion intensity versus
initial energy for various atomic and molecular singly and multiply
charged species. This figure clearly shows that on the higher energy
side the number of molecular species falls off drastically. There-
fore, if only those secondary ions with energies greater than 100 eV
are measured, the problem of molecular species interference is greatly
reduced. Fig. 4-6[9] shows the complex nature of the mass/electronic
charge spectrum in SIMS and also shows the advantage of employing a
spectrometer with greater mass resolution.

The influence of the incident ion on the surface is an important
characteristic in the qualitative and quantitative analysis of mater-
ials. The major influence that the primary ion beam energy has on the
sample is through the change it produces in the secondary ion yield.
The primary ion density changes the equilibrium concentration of ac-
tive species adsorbed on the surface and subsequently produces a
change in the secondary ion yield. The chemical character of the in-
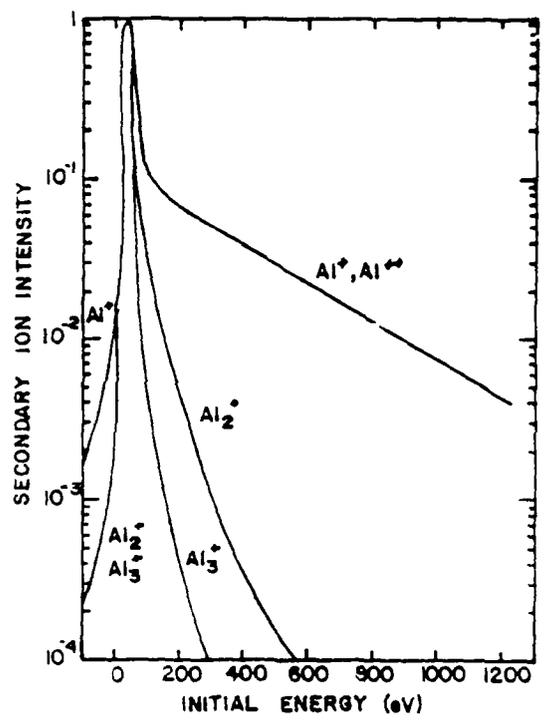
Figure 4-5 Energy distributions for various Al secondary
ion species sputtered from an Al-Mg alloy by
12 keV Ar$^+$. (ref. 7).
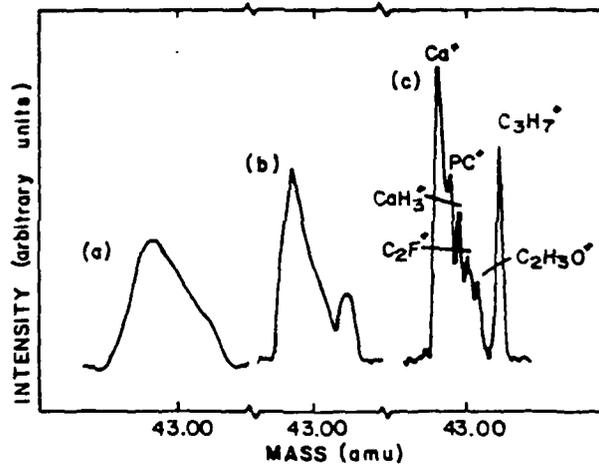
Figure 4-6 The mass 43 position of the secondary ion mass
spectrum of fluorapatite at an approximate mass
resolution of (a) 300, (b) 1000, and (c) 3000.
(ref. 7).

cident ion has little influence on the secondary ion yield if the dose is kept small (less than 10^4 ions cm^{-2}) because the amount of time to analyze the surface is small compared to the time that the incident ion significantly affect the surface.

The use of different incident ions affects the quality of the SIMS spectrum. Some of the usual ion beams employed are He^+, Ar^+, Ne^+, Xe^+, O^-, O_2^-, N_2^+, and Cs^+. Each ion beam has a particular advantage over the others. For example, the use of O^- enhances the emission of positive secondary ions and Cs^+ enhances the emission of negative secondary ions. Also the use of negative ion bombardment reduces surface charging so that insulators may be studied more readily. The degree of surface charging depends upon the ion species, charge, energy and current density, the dimensions of the bombarded area and the conductivity of the insulating surface. Again the same techniques used in ESCA experiment can be used in the SIMS experiment to reduce the problem of surface charging of insulators. However, the amount of information gained from the use of SIMS for the investigation of insulators is not sufficient to warrant the use of SIMS in this area.

Depth profiling by SIMS is another inherent advantage of SIMS for surface analysis. In SIMS the secondary ion signal is continuously measured as a function of the sputtering time. The sputter time can be related to the depth through experiments where a known film thickness is deposited on a different substrate and the secondary ion yield is monitored as a function of the time. The major problem in depth profiling is that the change in secondary ion signal is not al-

ways a measure of concentration changes. The fact that the ion beam causes uneven sputtering, edge effects, mixing, redeposition, and ion migration changes the secondary ion yield from the surface as a function of depth. Fig. 4-7[8] shows some of the major problems in the use of SIMS as a depth profiling analysis technique. These problems fall into two major categories, instrumental factors and ion-matrix effects.

The instrumental problems come from the fact that the current density incident on the sample is not uniform across the diameter of the beam and consequently there is nonuniform sputtering. Therefore, edge effects become much more pronounced the deeper into the matrix that SIMS analysis goes. One approach to the problem is to defocus the primary ion beam to an area much larger than the acceptance angle of the spectrometer so that a well defined area of uniform current density is established over the surface of analysis. However, the defocusing of the primary ion beam over the sample causes some back-ground effects due to the emission of secondary ions from areas out-side of the crater. The most effective means of eliminating problems in depth profiling is to raster the primary ion beam so that the cra-ter bottom is more uniform.

The ion-matrix effects are more pronounced in depth profiling with SIMS. The most important effects are the atomic mixing of sub-surface layers because of the implantation of primary ions as well as ions from the edges. The presence of both the implanted primary ions and recoil ions affects the secondary ion yield and consequently the intensity of the signal.
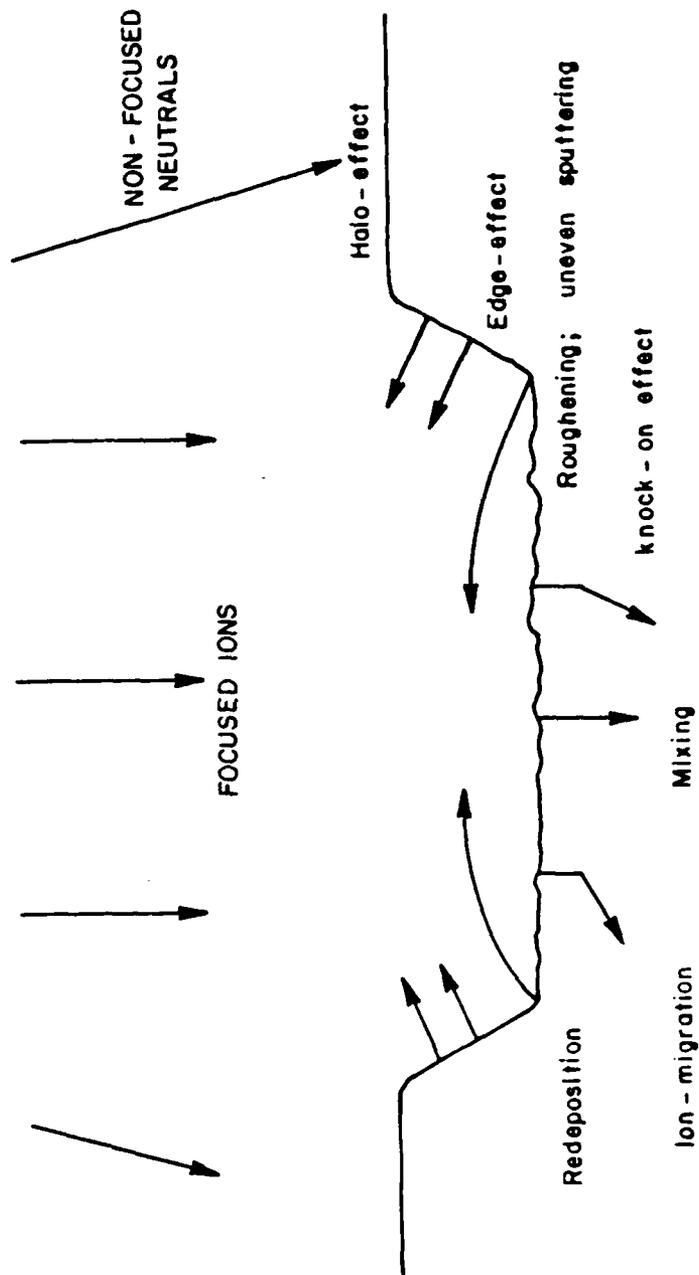
Figure 4-7 Effects of incident ion beam on sample surface. (ref. 8).

LIST OF REFERENCES

1. H. W. Werner, "Theoretical and Experimental Aspects of Secondary Ion Mass Spectrometry," Vacuum, 24, 493, (1975).

2. H. W. Werner, "The Use of Secondary Ion Mass Spectrometry in Surface Analysis," Surface Science, 47, 301, (1975).

3. A. Benninghoven, "Developments in Secondary Ion Mass Spectroscopy and Applications to Surface Studies," Surface Science, 53, 427, (1973).

4. A. Benninghoven, "Surface Investigation of Solids by the Statical Method of Secondary Ion Mass Spectrocopy (SSIMS)," Surface Science, 35, 427, (1973).

5. J. W. Coburn and E. Kay, "Surface Analysis Today," Research/ Development, December, 1972, 34, (1972).

6. A. van Oostrom, "Review of Surface Analysis Techniques," Proceeding from the VIII International Symposium on Discharges and Electrical Insulation in Vacuum, Albuquerque, New Mexico, 1978, CI.

7. A. W. Czanderna, ed., Methods of Surface Analysis, (Elsevier Scientific Publishing Company, New York, 1979), 223.

8. Presented by C. G. Pantano in a short course at the University of Dayton, Dayton, Ohio, on Techniques for Surface Analysis, (9 June 1980).

Chapter 5

Ion Scattering Spectrometry (ISS)

As noted in the previous chapter dealing with Secondary Ion
Mass Spectroscopy, one possible event that can occur when an ion is
incident on a target is the reflection of the ion. In Ion Scatter-
ing Spectrometry[1,2,3] (ISS) a low energy monoenergetic beam of ions
is incident upon the target. Some of these ions are reflected from
the surface and the energy of the reflected ions is measured. The
energy spectrum obtained provides information on the mass, and the
density of surface atoms. When ions with energy in the range of ap-
proximately 0.1-10 keV strike the surface, the scattering of these
ions occurs from mainly the outer atomic layer. Ions scattered from
atoms below the first monolayer are neutralized in the target. The
efficiency of detection of the back-scattered ion depends mainly upon
the cross-section for ion-atom interactions and on the neutralization
efficiencies of the surface being analyzed.

Because the energy of the ions used in ISS is low, a basic assump-
tion that is made is that the peaks observed in ISS are the result of
single binary elastic collisions[4]. Fig. 5-1 shows the model that
is assumed for ions incident on a surface. Using the laws of conser-
vation of energy and momentum the following expression for the ratio
of the scattered energy to the incident energy can be found

$$\frac{E_1}{E_o} = \frac{M_1^2}{(M_1+M_2)^2} \left(\cos\Theta_L + \frac{M_2^2}{M_1^2} - \sin^2\Theta_L \right)^2 , \tag{1}$$

where

M_1 = mass of primary ion

M_2 = mass of target atom
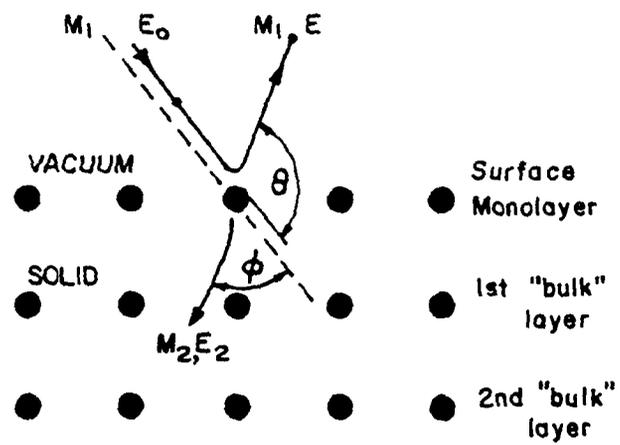
Figure 5-1 Model which describes interaction of low energy
ions with surface targets. (ref. 4).

E_1 = scattered ion energy

E_0 = incident ion energy

θ_L = scattering angle

For normal incidence this equation reduces to

$$\frac{E_1}{E_0} = \frac{M_2 - M_1}{M_2 + M_1}$$

Therefore, by measuring the ratio of the scattered energy to the incident energy of the ion the mass of the target atom can be calculated and the atom identified. Or by the use of tables of the energy ratios for a particular scattered species the target atom can be identified. One such table is published in the Handbook of Chemistry and Physics[4], 56th edition, for the scattering of ^{3}He, ^{4}He, ^{20}Ne and ^{40}Ar at $138°$.

The use of noble gas ions is mandatory in ISS if one is to obtain useful information about the surface composition of the target. David D. Smith[5] has shown that using reactive gas ions, such as 0^-, results in significant changes in the spectra of similar targets. His experiments showed that with the use of reactive gas species a large number of spikes occurred on the spectrum with energies significantly different than those predicted by Eq. (1). Since the penetration probabilities for the reactive species he used were similar to those of the noble gases he concluded that when using reactive species there is a much greater probability for surface neutralization processes, mainly due to surface effects, such as neutralization of the ion by Auger-like processes. However, even though the amount of neutralization of the scattered ions plays an important role in the quantitative analysis by ISS, it also serves to reduce the broadening of the backscattered peaks. As the ions

leave the surface they experience neutralization. Although not well understood, this phenomenon helps reduce the intensity of the peak on the low energy side, thus improving the resolution and sensitivity of the ISS spectrum. The degree of neutralization is dependent upon the energy of the reflected ion. Fig. 5-2[1] shows the ISS spectrum of polycrystalline gold at various incident energies and confirms the fact that the resolution is better for lower energy incident ions.

Quantitative analysis[6] by ISS is extremely complicated and not very reliable because little is known about the cross-sections for ion-atom interactions and the neutralization process is also not well understood. The intensity of a peak in the ISS spectrum can be written as:

$$I_i = I_o \; \theta_i N_o \; \sigma_i(E) \; \eta R,$$

where

I_i = scattering ion intensity from ith species,

I_o = incident ion intensity,

θ_i = fraction of surface sites occupied by ith species,

N_o = atoms/cm^2,

$\sigma_i(E)$ = scattering cross-section for ith species at energy E,

η = neutralization probability,

R = roughness factor.

The difficulty in quantitative analysis is related to the scattering cross-section. Fig. 5-3[5] shows the dependence of the differential cross-section as a function of the primary energy for He$^+$ on a copper crystal. The cross-section shows a sharp drop with increasing incident energy after a peak. The shape drop has been interpreted in
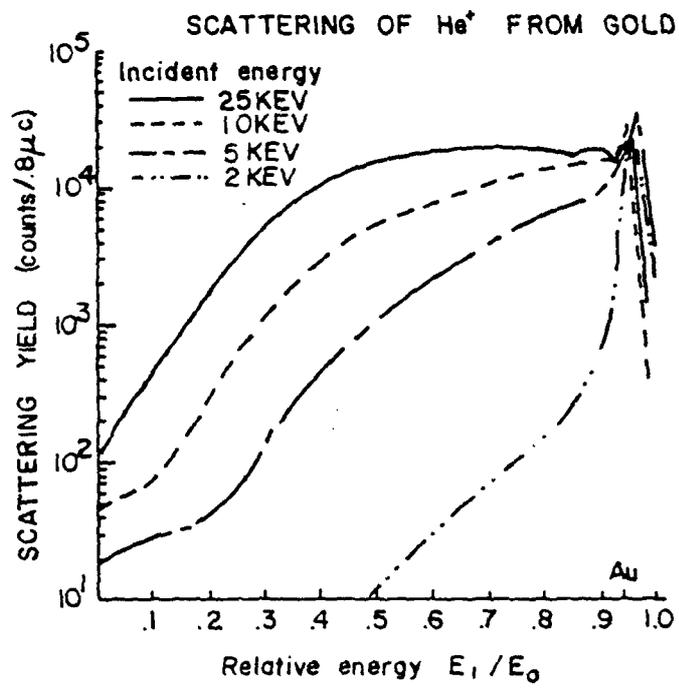
Figure 5-2 Spectra of $^4He^+$ backscattered from polycrystalline gold at various incident angles. (ref. 1).
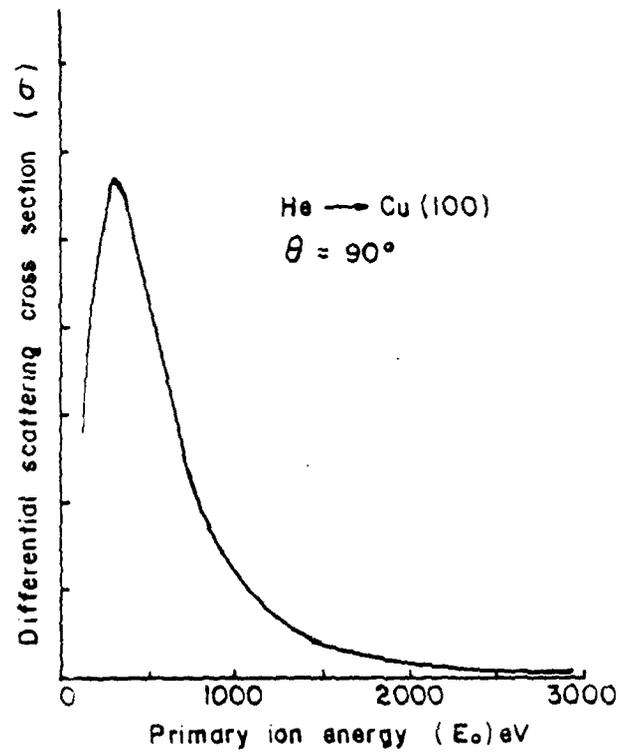
Figure 5-3 Plot showing dependence of ion scattering
          probability on primary ion energy for He
          bombarding Cu(100). (ref. 5).

terms of the neutralization probability by Cobos, Lamb, and Hag-

strum[7]. They predict that the probability that an ion will be neu-

tralized depends upon the velocity of the incident ion normal to the

surface and a characteristic velocity of the ion-metal surface. The

relationship they give for the cross-section is

$$\sigma_i = P_i \sigma_n,$$

where σ_i is the measured ion cross-section shown in Fig. 5-3, σ_n is

the cross section for scattering as a particle without regard for

charge exchange, and P_i is the probability that an ion is not neutral-

ized:

$$P_i \simeq A\exp(-v_o/v)$$

where v_o is the characteristic velocity of the ion metal surface, v is

the velocity of the incident ion, and A is a constant. Using these

equations they have been able to adequately predict the behavior of the

differential cross-section. The cross-section data they have accumula-

ted predicts that there is an energy which produces a maximum scatter-

ing signal for a given element. However, this energy is different for

each element and therefore values of the cross-section will be differ-

ent for different elements in the same target. The neutralization

probability they give is only a simple model and for many targets the

calculation of the characteristic velocity of the ion-metal surface

may be very complicated.

Another method for calculation of the cross-section[8] is to as-

sume a reasonable interaction potential between the ion and surface

and, through classical mechanics, calculate the cross-section. One

such calculation assumes the Bohr screened Coulomb potential for the

interaction potential. In this approach the potential is described by:

$$V(r) = \frac{Z_1 Z_2}{r} \; e^2 \; \exp\left(\frac{-r}{a}\right)$$

where

r = nucleon separation,

$a = a_0{}'(Z_1{}^{2/3} + Z_2{}^{2/3})^{1/2}$ is the electron screening length,

$a_0 = 0.53\overset{\circ}{A}$, the radius of the first Bohr orbit.

Tables of the results for differential cross-sections assuming this potential were published by Everhart, et. al.[9]

The problem of differential cross-sections is still an unsolved one as is the problem of the neutralization probability. Until further work can be done to solve these problems, the only method of quantitative analysis with ISS is through the calibration of scattered ion intensity with relative sensitivity factors. However, the use of relative sensitivity factors is still dependent upon the cross-sections and neutralization probabilities and cannot give accurate results.

Sputtering of the surface can be a problem in the analysis of materials by ISS. During the initial stages of the analysis a large peak is usually observed in the spectrum. This peak can be attributed to the sputtering of particles from the surface which have been adsorbed by the material. These peaks can be a problem because they often interfere with the primary scattered peaks. However, once the adsorbed particles have been sputtered away the spectra do not exhibit this phenomena. Sputtering is also inherent in ISS because of the characteristics of the incident ion beam. In order to minimize sputtering of the sample

surface, helium ions should be used in conjunction with a large surface area of the sample. For example, if the sputtering yield is unity, then 10^{15} ions/cm^2 are required to remove one monolayer of surface atoms. Assuming a measuring time of 10^3/seconds with a primary ion current density of 10^{10} ion/cm^{2}sec, the total dose will be 10^{13} ions/ cm^2 and only 10^{-2} monolayers will be removed. This limits the sensitivity of ISS because the scattered ion current density will be only 10^5 ions/cm^2 sec and the background at this level is appreciable. Sputtering is also used for depth profiling for which higher primary ion currents must be used. The same problems in analysis of sputtered surfaces seen in SIMS are also prevalent in ISS.

Double and multiple scattering may contribute additional features to the ISS spectrum. These features can arise from a variety of causes such as scattering by impurity ions from the surface and multiple ionization of bombarding ions. The double scattering of an ion before it enters the energy analyzer is best shown by Fig. 5-4[10]. The shoulder on the main peak is the result of double scattering which is a low probability event. Another interesting phenomenon is scattering from single crystal surfaces. However, since the work done in our laboratory is on amorphous materials these effects will not be treated. The phenomenon of double scattering is a consequence of primary ions penetrating into the surface without being neutralized, then these scattered ions will appear in the spectrum at a lower energy.

Shadowing effects are a possible means of determining the orientation of different surface species on a substrate. Shadowing occurs when the peak of one element is suppressed because another element
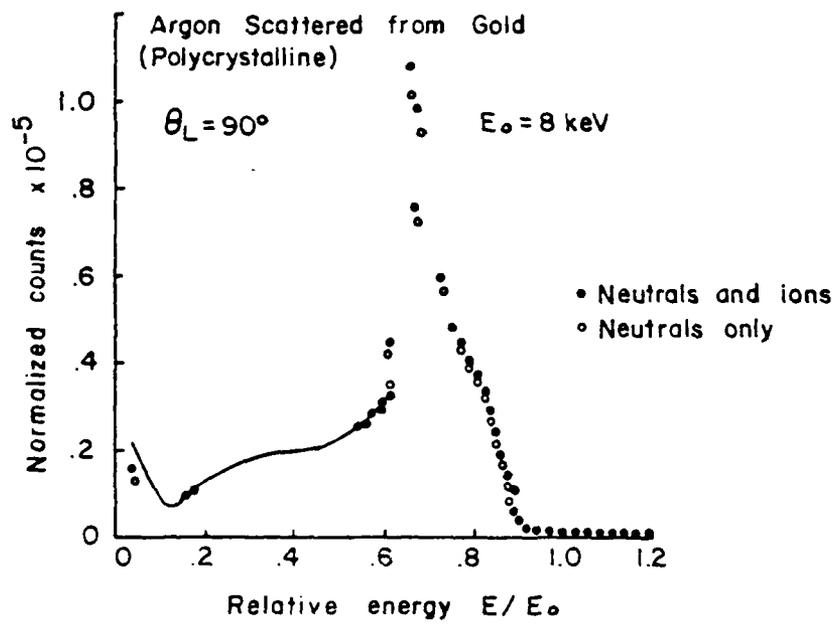
Figure 5-4 Energy spectra, derived from time of flight spectra,
for Ar scattered from polycrystalline gold. (ref. 10).

lies above it. So far the use of ISS for this purpose has not been exploited. Low Energy Electron Diffraction is a technique which has been used successfully for the identification of the surface orientation of molecules adsorbed on the surface.

Another feature of the ISS spectra, which may serve to elucidate surface structure, is changes in the peak width. Changes in the peak width can be attributed to an energy spread of the ion source due to geometry or to an angular spread which is a function of the optics used to analyze the scattered ions. Other influences on the peak width are surface roughness, thermal vibrations of surface atoms, and isotope effects. The thermal vibration effects can be used to calculate average vibrational energies of different surface atoms if it is possible to differentiate between the various peak broadening effects. Fig. 5-5[11] shows some of the additional information obtained in the ISS spectrum which may be useful in identifying surface features.

ISS is basically a surface analysis technique to be used on conductors, however, insulators may be analyzed with ISS. The problem in anlayzing insulators is surface charging. The sample surface gains a net positive charge because of the bombardment with the positive noble gas ions and because of the emission of highly energetic secondary electrons from the surface. Flooding the surface with electrons from a flood gun helps to neutralize the surface so that analysis of insulators is possible, however, the analysis of the spectrum may be too complicated[12].

ISS for surface analysis is quite useful for qualitative and semi-quantitative analysis of many materials. It is particularly useful
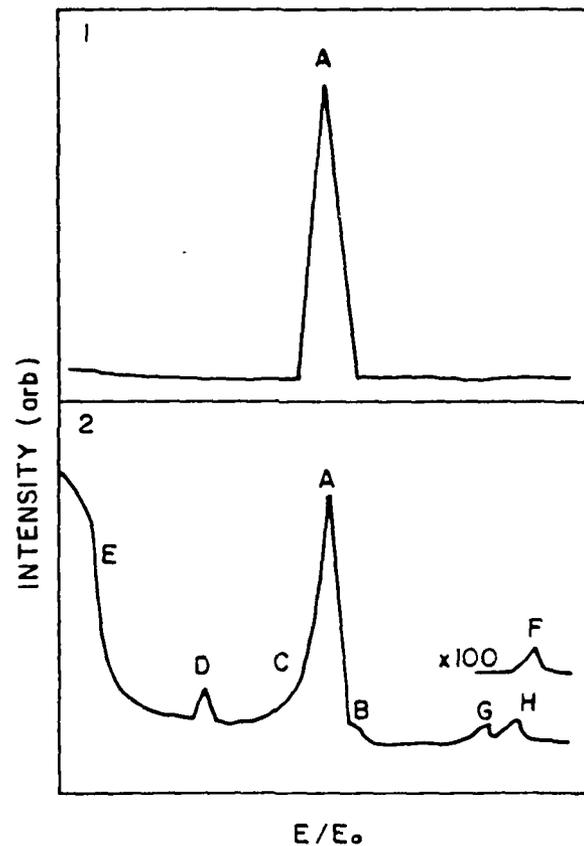
Figure 5-5 Summary of ion scattering effects: (1) Idealized binary scattering curve. (2) Spectral features recorded in practice from some materials (A) binary peak, (B) double scattering peak, (C) tailing inelastic peak, (D) sample impurities, (E) sputtered peak, (F) M_1^{++} scattering, (G) memory effects of earlier gases and (H) hydrogen impurity. (ref. 11).

for the analysis of materials where monolayer depth sensitivity is
desired. The quantitative analysis of materials by ISS is still an
unresolved problem, but once more standards have been published, cali-
bration of ISS for quantitative analysis will become much more useful.

LIST OF REFERENCES

1. A. W. Czanderna, ed., Methods of Surface Analysis, (Elsevier Scientific Publishing Company, New York, 1979), 75.

2. D. P. Smith, "Scattering of Low Energy Noble Gas Ions from Metal Surfaces," Journal of Applied Physics, 38, 340, (1967).

3. H. H. Brongersma and P. M. Mul, "Analysis of the Outermost Atomic Layer of a Surface by Low-Energy Ion Scattering," Surface Science, 35, 393, (1973).

4. Presented by C. G. Pantano in a short course at the University of Dayton, Dayton, Ohio, on Techniques for Surface Analysis, (9 June, 1980).

5. D. P. Smith, "Analysis of Surface Composition with Low-Energy Backscattered Ions," Surface Science, 25, 171, (1971).

6. H. Niehus and E. Bauer, "Quantitative Aspects of Ion Scattering Spectrometry," Surface Science, 47, 222, (1975).

7. A. Cobas and W. E. Lamb, "On the Extraction of Electrons from a Metal Surface by Ions and Metastable Atoms," Physical Review, 65, 327, (1944).

8. D. J. Ball, T. M. Buck, D. McNair, and G. H. Wheatley, "Investigation of Low-Energy Ion Scattering as a Surface Analytical Technique," Surface Science, 30, 69, (1972).

9. E. Everhart, G. Stone, and R. J. Carbone, "Classical Calculation of Differential Cross-sections for Scattering from a Columb Potential with Exponential Screening," Physical Review, 99, 1287, (1955).

10. T. M. Buck, W. E. Van der Weg, Y. S. Chi, and G. H. Wheatley, "Energy Spectra of 6-32 keV Neutral and Ionized Ar and He Scattered from Au Targets; Ionized Fraction as Functions of Time," Surface Science, 47, 244, (1975).

11. W. L. Baun, "Fine Features in Ion Scattering Spectra (ISS), Applications of Surface Science. 1, 81, (1977).

12. P. F. Kane and G. B. Larrabee, ed., Characterizatons of Solid Surfaces, (Plenum Press, New York, 1974), 627.

Chapter 6

Analysis by X-Ray Fluorescence (XRF)

X-rays emitted from a sample may be generated through bombardment by electrons, protons, and other x-rays, etc. However, in x-ray fluorescence (XRF)[1] analysis, the term fluorescence refers to those photons emitted from materials bombarded by photons. In XRF, x-rays impinge upon the surface of a sample causing the emission of an inner shell electron, leaving a vacancy that may be filled by an outer shell electron. This leads to some finite probability that an x-ray or Auger electron with an energy characteristic of the atom excited, will be emitted. The x-ray photon will have an energy that is related to the energies of the electron shells involved in the process. The analysis of these x-rays constitutes the technique of x-ray fluorescence.

When x-rays impinge upon a material there is a probability of absorption given by

$$I_t = I_o \exp(-ut) \tag{1}$$

where

I_t = transmitted intensity,

I_o = incident intensity,

u = mass absorption coefficient,

t = thickness of sample.

The mass absorption coefficient, which is the most important parameter in the determination of the attenuation of the incident radiation, is tabulated in many references[2]. By adding the weight fraction of an element multiplied by its mass absorption coefficient to the weight fraction of a second and/or third element multiplied by its mass absorption coefficient it is possible to determine the mass absorption of the entire com-

78

pound. Since the mass absorption coefficients are additive it is pos-
sible to determine the thickness of the material through which the x-
rays are absorbed, if knowledge of these coefficients is available and
if the elemental composition of the material is known. The mass absorp-
tion coefficient is a mixture of three different components: the photo-
electronic absorption component, which is a measure of the probability
of ionizing the atom with the incident radiation leading to the possible
emission of a characteristic x-ray; the coherent scattering coefficient;
and the incoherent scattering coefficient. The latter two parts of the
mass absorption coefficient contribute almost entirely to the background
level by scattering the incident radiation into the detector. To some
degree they contribute to some characteristic peak broadening by Compton
scattering effects. The mass absorption coefficient also determines
whether or not a generated photon can escape depending on the depth at
which it is emitted.

The fluorescence yield is another extremely important parameter. It
is a measure of the probability that an x-ray will be emitted when a hole
is created in an atom. Fig. 3-1 is a measure of the probability of x-ray
fluorescence versus emission of an Auger electron. Most of the insula-
tors used in high voltage spark gaps are composed of low-Z elements for
which the fluorescence yield of characteristic x-rays is practically zero.
Therefore, the technique of x-ray fluorescence applied to these insula-
tors is of little value, since the intensity of the emitted characteristic
x-rays will be shadowed by the background scattering of the incident ra-
diation. However, Richard Ryon and John Zahrt at Lawrence Livermore Lab-
oratory have developed a technique to solve this problem. They have de-

eloped a system whereby this background scattering from the material is greatly decreased by polarizing the incident x-rays. This increases counting time on the peaks of interest and the problem of low fluorescence yields is virtually elimated. It must be noted that in conventional x-ray fluorescence this sophisticated technique is not presently employed.

An attractive feature of x-ray fluorescence is that when characteristic x-rays are emitted from the valence levels they show intensity, wavelength, and line-shape changes which depend on the surrounding chemical structure[1]. The wavelength shifts are caused mainly through energy level changes due to shielding or screening of the electrons when the valence electrons are drawn into a bond. However, the shifts observed in the wavelength are not as great as the shifts measured by ESCA because the shifts observed in the characteristic x-rays are second order effects, measuring only energy level differences. The shape of the characteristic x-ray peak gives information on the energy distribution of the electrons occupying positions in or near the valence shell. However, theoretical calculations and predictions of electronic states from the shape of the lines are extremely complicated and highly speculative.

Finally, intensity changes in some lines due mainly to increases or decreases in the excitation probability of a given level are observed for characteristic x-rays emitted in the valence band. These increases or decreases in transition probabilities may be the result of a change of the character of the electron upon binding. The possibility of nonradiative transitions could also lead to intensity changes.

In XRF, photon energies in the 10-100 keV range are usually employed for the incident radiation. Since the region from which x-rays can be de-

tected determines the effective analysis volume of the specimen,
the use of XRF seems unattractive if one believes that the effective
damage range to be analyzed is only a few 100 $\overset{\text{o}}{\text{A}}$. A photon of 10 keV
can cause the emission of a characteristic x-ray from a depth of 1-2
μm. Multiple scattering of the penetrating x-ray beam in the material
causes the effective diameter of the analysis volume to be somewhat
larger than the beam diameter, which serves to distort the lineshape
of the detected characteristic x-rays.

An important technique in surface analysis is depth profiling.
In XRF, depth profiling is achieved by either sputtering the surface
away or by angle resolved measurements. With either technique prob-
lems still arise because of the sputtering process or the inherent
difficulties associated with XRF.

Because the amount of an element present in a material determines
the intensity of the emitted characteristic x-ray, a quantitative
analysis using XRF is possible. The intensity of the peaks is related
to the incident x-ray flux, the fluorescence yield of characteristic
x-rays, the ionization cross-section of an energy level by x-rays,
the density of atoms present, the mass absorption coefficient of the
material, the geometry of the analyzer system, and the geometry of
the x-ray source. Since most of these parameters are also character-
istic of other analytical techniques, quantitative analysis by XRF
is no more efficient than any other technique of surface analysis.

The use of XRF for the analysis of insulators is hindered by the
low fluorescence yield. However, the analysis of conductors does
not suffer from this same problem. The use of XRF for the analysis

of conductors can be a very useful tool. The use of polarized x-rays

can greatly increase the use of XRF as a surface analysis technique

and therefore needs to be investigated in greater detail. However,

until this problem can be solved the use of XRF for the analysis of

insulators is not profitable.

LIST OF REFERENCES

1.   P. F. Kane and G. B. Larrabee, ed., Characterization of Solid
     Surfaces, (Plenum Press, New York, 1978), 275.

2.   L. S. Birks, Electron Probe Microanalysis, (Wiley-Interscience,
     New York, 1971).

3.   R. W. Ryon, "Polarized Radiation Produced by Scatter for Energy
     Dispersive X-Ray Fluorescence Trace Analysis," Advances in X-Ray
     Analysis, 20, 575, (1977).

Chapter 7

Sputter Induced Photon Spectroscopy (SIPS)

The technique of Surface Composition by Analysis of Neutral and
Ion Impact Radiation (the common acronym is SCANIIR) or Sputter Induced
Photon Spectroscopy (SIPS)[1-2] is a surface sensitive technique for the
qualitative and semiquantitative analysis of both insulators and conduc-
tors. In this technique either ions or neutrals with energies less
than 4.0 keV are incident on the sample surface. The incident beam caus-
es the sputtering of neutral atoms, neutral molecules, and ions from
the surface. Some of these sputtered particles leave the surface in an
excited electronic state and subsequently emit optical radiation upon
decaying. The radiation emitted from the sputtered particles is character-
istic of the sputtered particles. Therefore, the surface constituents
can be qualitatively analyzed through the identification of the spectral
lines.

There are a number of problems that must be resolved before SIPS
can become a useful surface analysis technique[1]. First, the use of
neutrals as the incident radiation reduces the surface charging problem
of insulators. However, the creation of monoenergetic neutrals is com-
plex and inefficient process. Second, the sputtering process is not a
well understood phenomenon as was shown in the discussion of SIMS. Third,
the spontaneous decay processes which lead to the observed radiation, are
not well understood[3]. Thus, with SIPS only semiquantitative analysis
is possible. Finally, SIPS is a relatively new surface analysis tech-
nique that is still being investigated by experimentalists. Consequent-
ly, the mechanisms involved in the SIPS experiment are not well under-
stood.

There are three types of processes which may contribute to the photon emission. First, the incident particle may be excited as it is scattered by the surface. The excited particle will generally decay via the emission of a photon sufficiently far from the surface so that it is no longer influenced by the surface. Consequently, the radiative decay process is that for an isolated atom. A second process is the sputtering of excited target atoms from the surface, which can decay via the emission of a photon. A third process occurs when the detected photon is emitted within the surface itself. These photons are influenced by the surface properties of the material and may give some information on the chemical environment of the surface. A typical radiation spectrum produced by the SIPS experiment is shown in Fig. 7-1[1]. The observed emission line is Doppler-shifted and broadened, due to the wide range of energies and directions of the backscattered particles from the surface. The small peak on the high energy side is mainly due to photons reflected from the surface. The dotted line corresponds to the unshifted line and its resolution is generally determined by the resolution of the spectrometer. There have been many theoretical attempts to explain the shape of the peak seen in Fig. 7-1. One of the best theoretical calculations has been published by C. Kerkdyk and E. W. Thomas[3]. The third process is best seen when insulating targets are bombarded with low-Z projectiles. A typical example is shown in Fig. 7-2[1]. Neutral bombarding species are used rather than ions in order to avoid ion-beam defocusing effects and energy decreases due to charge build-up on the insulator surface. In all cases of insulators being bombarded with low-Z particles high intensity broadband radiation is detected.
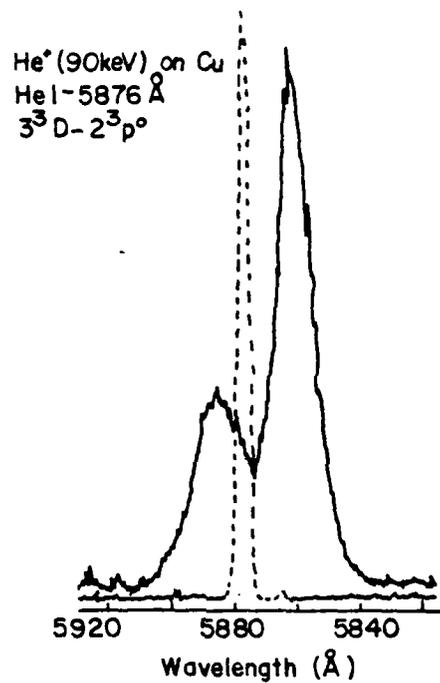
Figure 7-1 Measured line profile of HeI 5876 A produced in
the impact of He$^+$ (90 keV) on copper. The measured
line profile is indicated by the solid line. The
position of the unshifted line and the instrumental
resolution is indicated by the dotted line. (ref. 1).
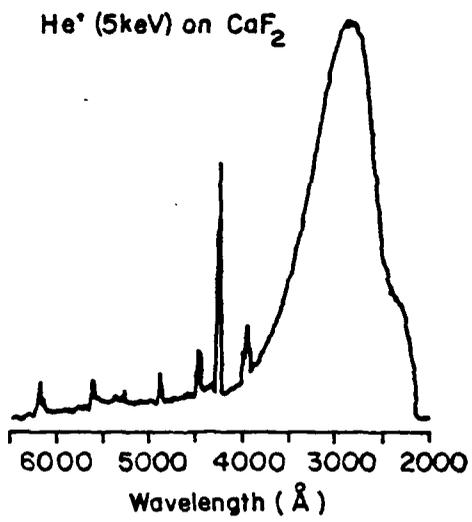
Figure 7-2 Spectrum of radiation produced in the impact
of He atoms (5 keV) on CaF_2. (ref. 1).

There is no proven means of accounting for this radiation, however, C. W. White, D. L. Simms and N. H. Tolk[1] seem to feel that the peak is a result of the radiative recombination of holes and mobile electrons created by the inelastic collisions of incident particles within the insulator surface.

Quantitative analysis with SIPS is extremely complicated due to the relaxation of excited species by non-radiative transitions[4]. If an excited atom is within a few angstroms of the surface, one-electron resonance processes and two-electron Auger processes are significantly more efficient than radiative decay for the relaxation of sputtered species. Thus, the intensity of optical lines is greatly decreased by these two processes. The non-radiative deexcitation probability for either of these two processes can be approximated by the following expression:

$$P(s) = Ae^{-as}$$

where P(s) is the non-radiative dexcitation probability,

A is the non-radiative transition rate at the surface,

a is a constant dependent on the surface material,

s is the distance away from the surface.

Values of "A" and "a" for a SiO_2 layer on a Si substrate are typically $A \sim 10^{15}$ /sec and $a \sim 2 \times 10^8$ cm.

The subsequent probability that an excited atom will escape the surface and radiate a photon is

$$R = \exp(-A/av_\perp)$$

where $v_\perp$ is the component of velocity of the sputtered atom normal to the surface. Therefore, a quantitative analysis with SIPS must take into account these two probabilities as well as the sputtering rates of particles

from the surface. The sputtering rate was considered in the chapter on SIMS and was shown to be the single largest deterrent to quantitative analysis by SIMS. Obviously, SIPS suffers from the same problems.

The use of SIPS for depth profiling is similar to that of SIMS. The spectrum of radiation is measured as a function of bombardment time. The bombardment time is then related to the depth of analysis only if the sputtering efficiency for the atom in the material matrix is known. Since the sputtering efficiency is such a complicated function of the material matrix, it can only be approximated from other experiments, such as SIMS.

Even though SIPS is an extremely sensitive surface technique it does suffer from many problems. Consequently, the use of SIPS to investigate the damage to various parts of spark gaps does not seem advisable at this time.

LIST OF REFERENCES

1. P. F. Kane and G. B. Larrabee, ed., Characterization of Solid Surfaces, (Plenum Press, New York, 1978), 641.

2. C. W. White, D. L. Simms, and H. H. Tolk, "Surface Composition Determined by Analysis of Impact Radiation," Science, 177, 481 (1972).

3. C. Kerkdijk and E. W. Thomas, "Light Emission by H and He Impact on a Clean Copper Surface," Physica, 63, 577, (1973).

4. C. W. White and N. H. Tolk, "Optical Radiation from Low-Energy Ion-Surface Collisions," Physical Review Letters, 26, 486, (1971).

Chapter 8

Scanning Electron Microscope (SEM)

The scanning electron microscope (SEM)[1] is a versatile tool for
the analysis of materials. It performs the functions of an optical micro-
scope, electron microscope, transmission electron microscope, Auger elec-
tron analyzer, and an x-ray fluorescence analyzer. Each of these analy-
sis techniques is performed in the same manner as described elsewhere in
this review and therefore a description of their use has been omitted
here. Also, the use of the scanning electron microscope is a well docu-
mented subject and the reader is referred to a number of excellent books
on the subject[2,3]. The SEM uses a beam of electrons as the incident ra-
diation. This beam of electrons when incident on a sample surface causes
the emission of secondary electrons, Auger electrons, and characteristic
x-rays. Each of these forms of radiation can be independently analyzed
in the SEM.

Since an SEM is located in the Geosciences Department at Texas Tech
University samples taken from various spark gap experiments will be analyz-
ed using the SEM. The main use of the SEM in this lab will be to locate
and identify defects in the surfaces of samples used in the spark gaps in
our laboratory.

LIST OF REFERENCES

1. P. F. Kane and G. B. Larrabee, ed., Characterization of Solid
   Surfaces, (Plenum Press, New York, 1974), 107.

2. P. R. Thornton, Scanning Electron Microscopy, (Chapman and Hall,
   London, 1968).

3. O. Johari, Scanning Electron Microscopy, (IIT Research Institute,
   Chicago, 1971).

Chapter 9

Profilometry

The profilometer[1] is a convenient means of investigating the topography of surfaces as well as some of the mechanical properties of surfaces. A sharply pointed stylus is placed on the surface to be investigated. It is then traversed across the surface while recording the up and down movement relative to a suitable mechanical standard. The stylus is defined by the American Standard of Surface Texture to be a pyramidal or conical diamond forming a 60° cone with a tip radius of 12.5 μ. The force applied to the stylus, which insures maintaining contact with the surface during movement, is defined as 0.0098nts multiplied by the tip radius in microinches squared. This is usually about 100 mg. The reason for the restriction to the force on the stylus is to insure that the surface is not mechanically damaged by the stylus and yet still maintains contact.

The stylus is connected to a transducer, and the fixed part of the transducer is connected by some mechanical means to a reference surface. Therefore any movement of the transducer relative to the reference surface is a direct result of movement of the stylus. The reference material is usually a smooth surface, long compared to the sample surface having deviations over the length of the surface small compared to those of the sample surface. The length of the surface usually measured in one sweep of the sample varies between 0.4 inches and 2.0 inches, with a speed of about 0.05 inches/sec.

The first requirement for the analysis of a sample is to establish a reference line on the test material. Once the reference line has been established it is necessary to determine what information from a profile

90

is relevant. Usually the most relevant parameter measured is Ra, which is the average value of the modulus of the deviations of the profile from the reference line. If there is any doubt the reliability of the information from one track of the surface, then more than one track should be taken and statistical limits put on the variations. This is especially the case if surface cracks are present on the sample.

Since the topography of the surface of a spark gap electrode influences the electric field strength at the surface, the topography of any scratches or craters on the surface must be investigated. Therefore, profilometry is a crucial tool for the analysis of conductor surfaces.

LIST OF REFERENCES

1.   P. F. Kane and G. B. Larrabee, ed., Characterization of Solid Surfaces, (Plenum Press, New York, 1974), 49.

Chapter 10

Photoacoustic Spectroscopy (PAS)

In photoacoustic studies of solids[1,2,3] a sample is placed in a
closed, gas-filled container. The sample is then illuminated with mono-
chromatic light chopped at a certain frequency. Absorption of the chop-
ped light by the sample causes periodic heating of the sample, which
results in a temperature variation in the sample. In a thin layer of
the gas adjacent to the sample, variations in the gas temperature result
in fluctuations in the gas pressure. These pressure fluctuations repre-
sent an acoustic signal, which is detected by a microphone in the cell
wall. The detection of the acoustic signal provides the basis for the
study of the optical absorption in the sample. The absorbed optical ener-
gy which causes the photoacoustic signal is that fraction of the total ab-
sorbed energy which is converted to heat via nonradiative de-excitation
processes in the sample. The photoacoustic signal corresponds to the op-
tical absorption spectrum of the sample as long as the nonradiative pro--
cesses dominate in the dissipation of the absorbed light energy.

Rosencwaig and Gusho[4] believe that the primary source of the acou-
stical signal received by the microphone is caused by the periodic heat
flow from the solid to the surrounding gas as the solid is cyclically
heated by the chopped light. They also believe that only a relatively
thin layer of gas can be thought of as an acoustic piston, which creates
the acoustic signal detected by the microphone. The periodic pressure
fluctuations in the cell are proportional to the amount of heat dissipated
in the solid absorber. Fig. 10-1[3] shows a cross-sectional view of a
cylindrical photo-acoustic cell.

Consider a sinusoidally chopped monochromatic light beam incident on
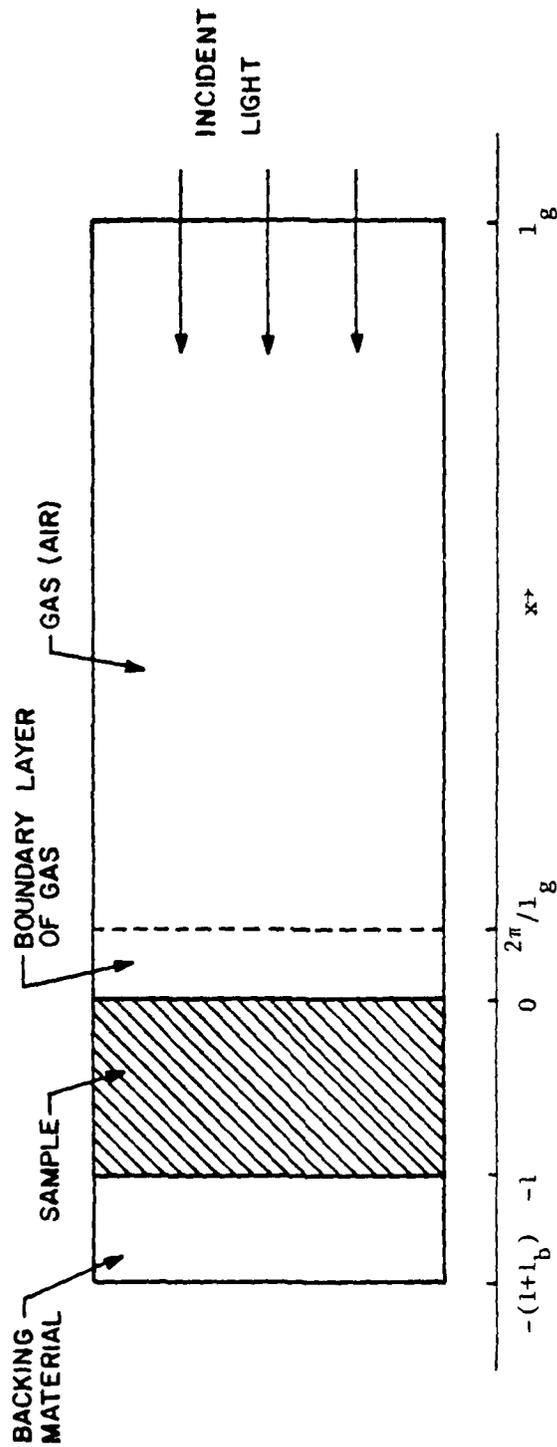
Figure 10-1 Cross-sectional view of a simple cylindrical photoacoustic cell, showing the positions of the solid sample, backing material, and gas column. (ref. 3).

the solid with an intensity given by,

$$I = \tfrac{1}{2}I_0(1 + \cos \omega t), \tag{1}$$

where I_0 is the incident monochromatic light flux, and ω is the chopping frequency of the incident light beam. Then the heat flux density produced at any point on the solid is given by

$$\tfrac{1}{2}\beta I_0 \exp(\beta x) (1 + \cos \omega t) \tag{2}$$

where β is the optical absorption coefficient of the solid. The thermal diffusion equation in the solid is given by,

$$\frac{\partial^2 \phi_s}{\partial x^2} = \frac{1}{\alpha s} \frac{\partial \phi_s}{\partial t} - A\exp(\beta x)[1 + \exp(j\omega t)] \tag{3}$$

for $-1 \leq x \leq 0$,

where

α_s = thermal diffusivity of the sample = $k_s/\rho_s C_s$,

ρ_s = density of the solid,

C_s = specific heat of the solid,

k_s = thermal conductivity of the solid,

$A = \beta I_0 \eta/2k_s$,

η = efficiency at which the absorbed light is converted to heat by the

nonradiative de-excitation processes.

The thermal diffusion equations for the backing and the gas are given by,

$$\frac{\partial^2 \phi_b}{\partial x^2} = \frac{1}{\alpha_b} \frac{\partial \phi_b}{\partial t} \quad \text{for } -1-1_b \leq x \leq -1 \tag{4}$$

and

$$\frac{\partial^2 \phi_g}{\partial x^2} = \frac{1}{\alpha g} \frac{\partial \phi_g}{\partial t} \quad \text{for } 0 \leq x \leq 1_g \tag{5}$$

where α_b and α_g are similarly defined as α_s in Eq. (3).

In principle these equations are extremely complicated to solve, therefore only the explicit solution for the amplitude of the periodic tempera-

ture variation at the solid-gas boundary will be given. The amplitude

of the periodic temperature variation at the solid-gas boundary is

$$\theta = \frac{\beta I_o}{2ks(\beta^2 - \sigma_s^2)} \left(\frac{(r-1)(b+1)\exp(\sigma_{s}l)-(r+1)(b-1)\exp(-\sigma_{s}l)+(2(b-r)\exp(-\beta l)}{(g+1)(b+1)\exp(\sigma_{s1})-(g-1)(b-1)\exp(-\sigma_{s1})} \right) (6)$$

where

$$b = \frac{k_b a_b}{k_s a_s} \qquad g = \frac{k_g a_g}{k_s a_s}$$

$$r = (1-j)\frac{\beta}{2a_s} \qquad a = \left(\frac{\omega}{2\alpha}\right)^{\frac{1}{2}} = \text{thermal diffusion coefficient of the solid.}$$

$$\sigma_s = (1+j)a_s \qquad \mu = \frac{1}{a} = \text{thermal diffusion length}$$

Due to the periodic heat flow from the solid to the boundary layer of

gas, the gas layer periodically expands and contracts causing an acou-

stic piston effect on the rest of the gas column. The displacement of

this acoustic piston is given by

$$\Delta x(t) = 2\pi\mu g \ \frac{\langle\phi_g(t)\rangle}{\phi_o(0)} \qquad (7)$$

where $\langle\phi_g(t)\rangle$ represents the temperature variation averaged over the

boundary layer, and $\phi_o(0)$ is the steady state temperature of the sample.

Using the adiabatic gas law ($PV^\gamma = $ constant, P = pressure, V = volume,

and $\gamma = $ ratio of the specific heats) the change in pressure of the gas

column is

$$\Delta P(t) = \frac{\gamma P_o}{1_g} \ \Delta x(t) \qquad (8)$$

where P_o is the steady state pressure of the photoacoustic cell. This

equation gives an approximate expression for quantitative analysis of

the photoacoustic signal.

A plane thermal wave in any medium has the general form

$\exp(j\omega t - \sigma x)$, where $\sigma = (1+j)\left(\frac{\omega}{2\alpha}\right)^{\frac{1}{2}}$. Therefore a plane thermal wave is

exponentially damped by a factor e^{-1} within one thermal diffusion

length, $\mu = (\frac{2\alpha}{\omega})^{\frac{1}{2}}$. For example, in one thermal wavelength, $\lambda t = 2\pi\mu$,

the amplitude is damped by a factor $\exp(-2\pi) \simeq 0.002$. Consequently,

any heat generated at a depth greater than λt will not significantly

contribute to the photoacoustic signal. Table 10-1[1] gives typical

values of the thermal diffusion length for some common materials. The

fact that the average value of the thermal diffusion length, μ, is

about 2×10^{-3}cm creates a problem in the analysis of some materials by

PAS. The reason the sampling depth in PAS is a problem is that mater-

ials such as lucite, nylon, and delrin, irradiated by ultraviolet ra-

diation, are probably damaged to depths from 50-500 A^{o}[5]. Since the

sampling depth in PAS is approximately 20 μm the photoacoustic signal

is representative of the undamaged bulk and not the damaged 50-500 Å.

The thermal diffusion length is proportional to the chopping fre-

quency[6], ω, and therefore it should be possible to obtain an acoustic

signal from a thin surface layer by changing the chopping frequency.

Since the thermal diffusion length is defined as $\mu = (\frac{2\alpha}{\omega})^{\frac{1}{2}}$, the frequency

required for an analysis depth of approximately 500 Å is given by

$\omega = 8 \times 10^{10} \alpha(cm^{-2})$. For aluminum, where $\alpha = 0.82$ cm^2/sec, the value

of ω for $\mu = 500$ Å is approximately 40.8×10^{10} rad/sec. For this val-

ue of ω the width of the acoustic piston, using air as the surrounding

gas, is approximately 4680 Å. This creates a variety of problems in

the analysis of thin layers by PAS. First, the frequency of the acou-

stic wave is approximately the same as the chopping frequency and there-

fore a microphone capable of detecting a 10^{10}Hz frequency is required.

The biggest problem is in the design of the photoacoustic cell. The

theory presented above assumes that the dimensions of the cell are

Photoacoustic Parameters for Various Substances (1)

TABLE 1

Substance	Density ρ (gm/cm^3)	Specific heat C (cal/gm-C)	Thermal Conductivity k (cal/cm-sec-C)
Aluminum	2.7	0.216	4.8×10^{-1}
Stainless steel	7.5	0.12	3.3×10^{-2}
Brass	8.5	0.089	2.6×10^{-1}
KCl crystal	2.0	0.21	2.2×10^{-2}
Crown glass	2.6	0.16	2.5×10^{-3}
Quartz	2.66	0.188	2.2×10^{-3}
Rubber	1.12	0.35	3.7×10^{-4}
Polyethylene	0.92	0.55	5×10^{-4}
Water	1.00	1.00	1.4×10^{-3}
Ethyl Alcohol	0.79	0.60	4.2×10^{-4}
Chloroform	1.53	0.23	2.9×10^{-4}
Air	1.29×10^{-3}	0.24	5.7×10^{-5}
Helium	1.80×10^{-4}	1.25	3.4×10^{-4}

Substance	Thermal diffusivity $\beta = k/\rho c$ (cm^2/sec)	Thermal diffusion length at 100 Hz. $\mu = (\frac{2\beta}{\omega})^{\frac{1}{2}}$
Aluminum	0.82	5.1×10^{-2}
Stainless steel	$3.7\text{x}.0^{-2}$	1.1×10^{-2}
Brass	0.34	3.3×10^{-2}
KCl crystal	5.2×10^{-2}	1.3×10^{-2}
Crown glass	6.0×10^{-3}	4.4×10^{-3}
Quartz	4.4×10^{-3}	3.7×10^{-3}
Rubber	9.4×10^{-4}	1.4×10^{-3}
Polyethylene	9.9×10^{-4}	1.8×10^{-3}
Water	1.4×10^{-3}	2.1×10^{-3}
Ethyl Alcohol	8.9×10^{-4}	1.7×10^{-3}
Chloroform	8.4×10^{-4}	1.6×10^{-3}
Air	0.19	2.5×10^{-2}
Helium	1.52	7.0×10^{-2}

small compared to the wavelength of the acoustic signal, an impossibility for this example.

Surface studies have been performed with PAS but the requirement for the use of PAS is that the sample be a film present on a substrate which is either highly reflective or extremely opaque to the optical radiation. However, because most of the materials to be investigated in this lab are not films on such substrates, surface studies by this method are not likely to be productive.

PAS has some advantages as a material analysis technique. For instance, photoacoustic spectroscopy can be performed on any material, whether it be crystalline, amorphous, power, smear, gel, etc. Also, acoustic spectra can give comparable optical absorption spectra even on materials that are opaque because the acoustic signal is proportional to the optical absorption coefficient. However, for the investigation of materials in our lab where the damage layer is much thinner than the analysis depth of PAS, the use of PAS would not be applicable.

LIST OF REFERENCES

1. A. Rosencwaig, "Photoacoustic Spectroscopy," Journal of Applied Physics,, 49, 2905, (1978).

2. A. Rosencwaig, "Photoacoustic Spectroscopy," Analytical Chemistry, 47, 592A, (1975).

3. A. Rosencwaig, "Photoacoustic Spectroscopy of Solids," Physics Today, 28, 23, (1975).

4. A. Rosencwaig and A. Gersho, "Theory of the Photoacoustic Effect with Solids," Journal of Applied Physics, 47, 64, (1976).

5. H. Yasuda, H. C. Marsh, S. Brandt, and C. N. Reilley, "ESCA Study of Polymer Surfaces Treated by Plasmas," Journal of Polymer Science: Polymer Chemistry Edition, 15, 991, (1977).

6. F. A. McDonald, "Photoacoustic Effect and the Physics of Waves," American Journal of Physics, 48, 41, (1980).

Chapter 11

Attenuated Total Reflection (ATR)

Attenuated Total Reflection[1-4] is a method of measuring the optical absorption spectrum of materials by introducing light into an optically transparent internal reflection element (IRE) at angles above the critical angle. After the light has suffered many internal reflections the intensity of the emerging light is measured. Fig. 11-1[5] shows the basic experimental setup for studying optical absorption by Attenuated Total Reflection (ATR). The sample is placed next to the internal reflection element (IRE) and light enters the IRE at angles greater than the critical angle striking the surface of the sample. Scanning through the optical radiation spectrum the sample absorbs energy at those wavelengths where other optical absorption spectroscopy techniques also exhibit absorption. The surface sensitivity of this method is due to the fact that electromagnetic waves actually penetrate a certain distance past the surface of the IRE and samples brought within this distance will interact with these fields, even if they are opaque.

The depth of analysis can be calculated using Fresnel's equations and is dependent upon the indices of refraction of the IRE, the sample and the backing material, the angle of incidence, the thickness of the sample, and the polarization of the incident radiation. The effective sampling depth is given by the equations:

$$de = \frac{4n_2 \, d\cos\theta}{1-n_3^2}$$

$$de_{11} = \frac{4n_2 \, d\cos\theta [(1+n_{32}^4)(\sin^2\theta)-n_{31}^2]}{(1-n_3^2)[(1+n_{31}^2)\sin^2\theta - n_{31}^2]}$$

where n_{3x} = ratio of index of refraction of medium 3 to medium x
where x = 1,2

101
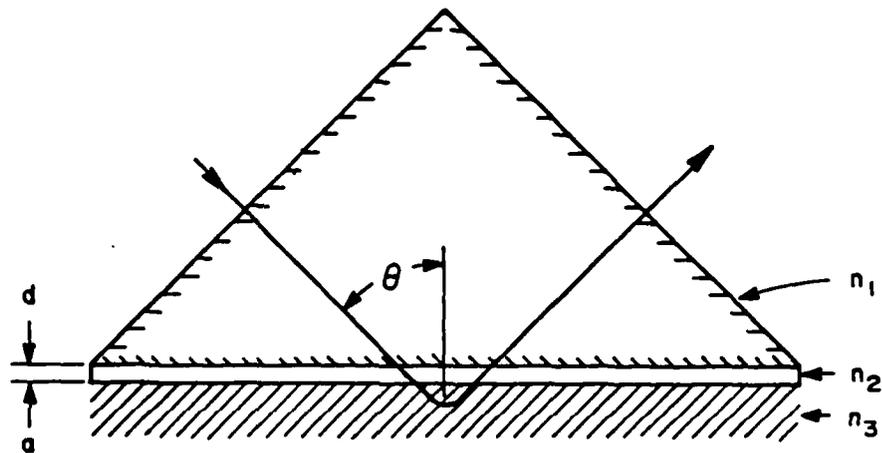
Figure 11-1 Schematic representation of the path of a ray of light
undergoing total internal reflection. The ray penetrates
a fraction of a wavelength beyond the reflecting inter-
face. Medium 1 is the optically transparent IRE, medium
2 is the sample material, the surrounding medium 3 is
usually air. (ref. 5).

where de and de_{11} are the sampling depths for light of perpendicular and parallel polarization relative to the reflecting surface of the IRE. The depth of analysis[1] is on the order of the wavelength of the incident radiation, which usually varies from 7000-10,000 Å. Two problems arise; first, if the sample is not in good contact with the IRE, because of variations in the topography of the sample, then the sampling depth will vary significantly. Also, even if the sample is in good contact with the IRE the sampling depth is considerably deeper than the anticipated depth of damage done to materials in our lab.

Another problem associated with the use of ATR for the investigation of materials that will be investigated in our lab, is that the material must be coated onto the IRE or be present as a thin layer on a highly reflecting substrate. Therefore ATR does not seem applicable to the analysis of the surfaces of insulators or conductors used in spark gaps.

LIST OF REFERENCES

1. Paul A. Wilkes, Jr., "Internal Reflection Spectroscopy," _American Laboratory_, June (1980), 92.

2. J. Fahrenfort, "Attenuated Total Reflection," _Journal of Molecular Spectroscopy_, 15, 701 (1962).

3. N. J. Harrick, "Study of Physics and Chemistry of Surfaces From Frustrated Internal Reflections," _Physical Review_, _Letters_, 4, 224, (1960).

4. N. J. Harrick, _Internal Reflection Spectroscopy_, (John Wiley and Sons, Inc., New York, 1967).

5. P. F. Kane and G. B. Larrabee, ed., _Characterization of Solid Surfaces_, (Plenum Press, New York, 1974), 215.

Chapter 12

Surface and Volume Resistivity

The measurement of surface and volume resistivities may provide useful information about the breakdown characteristics of insulators in high voltage spark gaps. One proposed theory[1-3] for the surface breakdown of solid insulators is that due to electrical stresses at the cathode-insulator junction, field-emitted electrons are produced which impinge upon the insulator surface. When these field-emitted electrons hit the insulator surface they produce additional electrons through secondary emission. Some of these secondary electrons strike the surface of the insulator producing still more electrons. Eventually, a cascade occurs which develops into a secondary electron emission avalanche along the surface of the insulator. The resistivity of the surface is an important characteristic in this process. It has been shown that the use of conductive coatings on the surface of insulators is helpful in the reduction of this avalanche process[4].

Two possible explanations for the apparent improvement in insulator performance because of the application of conductive coatings have been proposed[4]. First, the lower surface resistivity helps to alleviate the problem of charge buildup on the insulator surface. Second, the lower surface resistivity helps inprove the uniformity of a charge distribution on the surface which reduces the resultant electric stress on the insulator. Therefore, the measurement of surface or volume resistivity could be important in the analysis of insulators.

The measurement of surface and volume resistivity have been standardized by the American Society for Testing Materials. In our lab we

104

have a Keithley Model 6105 Resistivity Adapter which uses circular geometry as defined by the ASTM. Fig. 12-1 shows the circular geometry used in this resistivity adapter. The ASTM defines the volume resistivity as the ratio of the potential gradient parallel to the current in the material to the current density. Consequently, the volume resistivity, ρ, is given by

$$\rho = \frac{E}{J} \tag{1}$$

where E is the potential gradient between electrodes 3 and 1 and J is the current density in the material. This leads to an equation of the form

$$\rho = \frac{22.9V}{t_c\,I} \ \Omega\text{-cm} \tag{2}$$

where V is the potential between electrodes 3 and 1, I is the current through the material and t_c is the average thickness of the material. The surface resistivity is defined as the ratio of the potential gradient parallel to the current along the surface to the current per unit width of the surface. Therefore, the surface resistivity, σ, is given by

$$\sigma = \frac{E\omega}{I} \tag{3}$$

where E is the potential gradient between electrodes 2 and 1, ω is the width between electrodes 2 and 1, and I is the current between these two electrodes along the surface of the insulator. Consequently, the surface resistivity is given by

$$\sigma = \frac{53.4V}{I} \ \text{ohms} \tag{4}$$

Using this resistivity adapter and Eqs. (2) and (4) it is possible to measure both the volume and surface resistivity of most materials. One problem that occurs in using this method is that the size
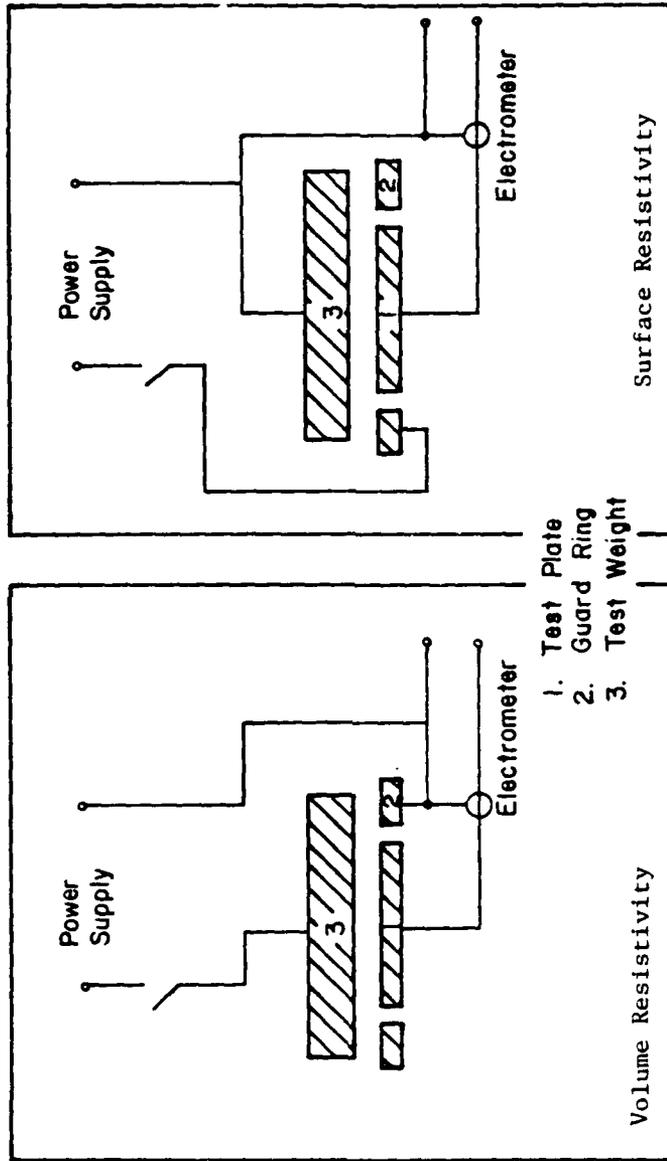
Figure 12-1 Simplified diagrams of Model 6105 resistivity adapter for volume and Surface resistivity measurement.

of the sample is limited to a circular disk of a maximum diameter of 2.5 inches and maximum thickness of .25 inches. The minimum values are 2.5 inches for the diameter and .0625 inches for the thickness. The reason for these limitations is that the thickness of the sample must be larger than the separation of the electrodes, to insure that the majority of the current flows along the surface of the insulator and not through the insulator. This is also a problem if the volume resistivity of the material is not much larger than the surface re-sistivity. Figures 12-2 through 12-5 show the surface and volume resistivity of some insulators being studied in our laboratory.

From the curves shown in these figures another problem arises. Apparently the resistivity of various insulating materials changes as a function of time. One theory for this change is that the measured current is made up of four different components: a normal charging cur-rent, a reversible absorption current, an irreversible absorption cur-rent, and a leakage conduction current[5]. Fig. 12-6 shows these four currents as a function of time. Each current affects the value of the resistivity in a different way.

The normal charging current arises from the polarization of the material. It is independent of the resistivity of the material, and dependent upon the capacitance and resistance of the external circuit. Therefore the amount of current produced from this effect is dependent upon the characteristic time involved in the external circuit. The other three currents act for a considerably longer time than the nor-mal charging current. By convention, since 1895, a 1-minute electrifi-cation time has been employed. This means that the surface resistiv-
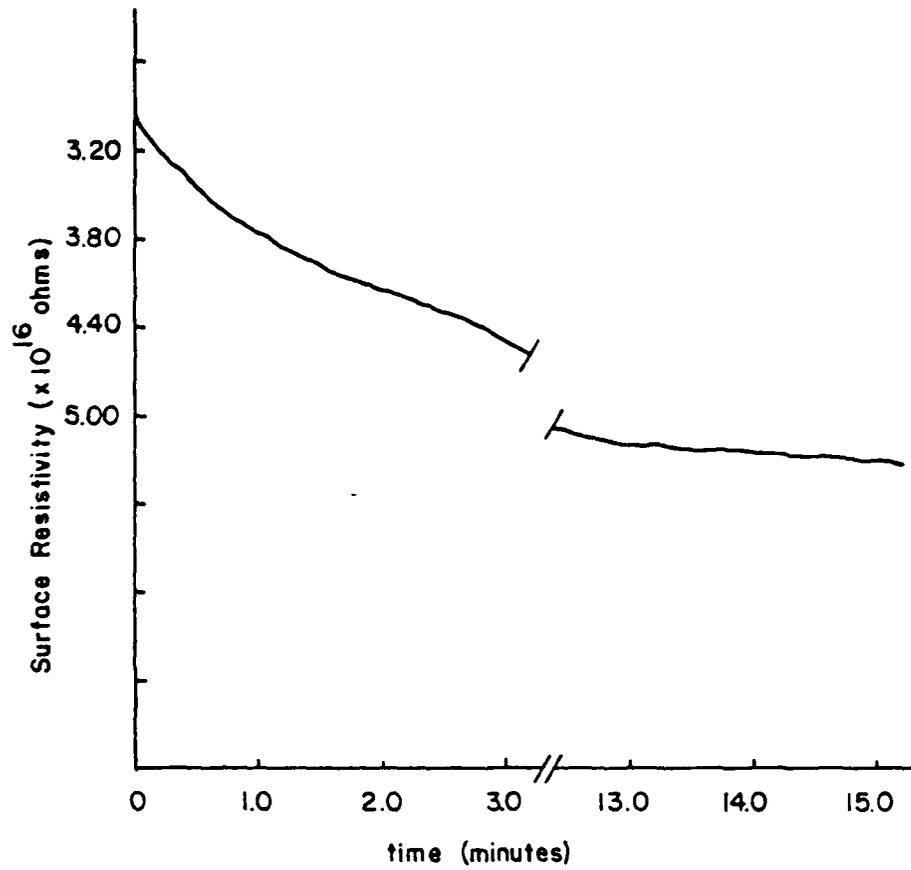
Figure 12-2 Surface resistivity of a Lucite sample (2.5" diameter
by .125" thickness) at 500 volts.
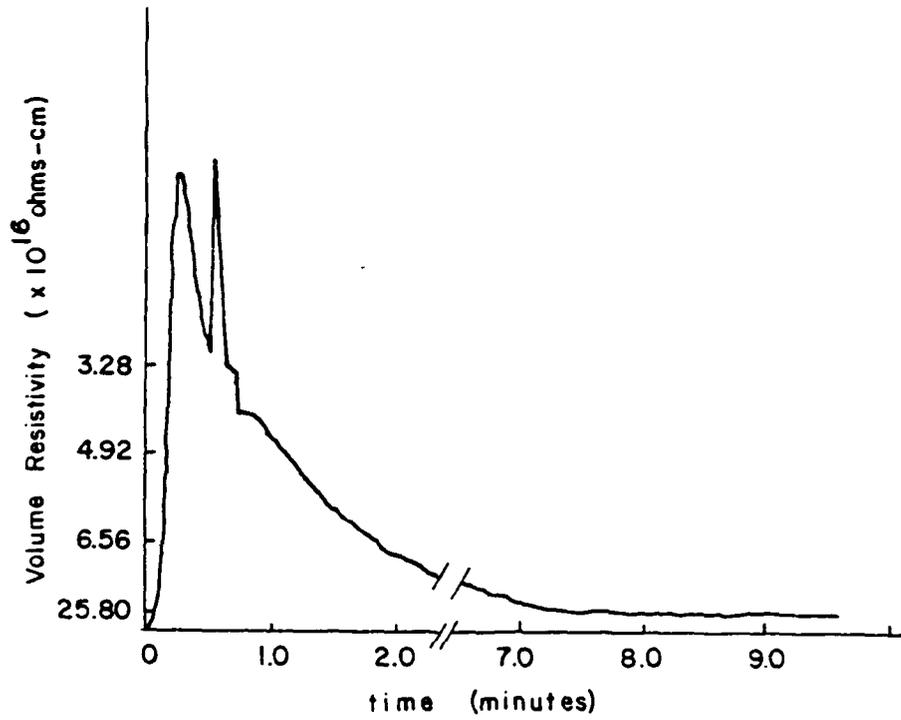
Figure 12-3 Volume resistivity of a Lucite sample (2.5" diameter
by .125" thickness) at 500 volts.
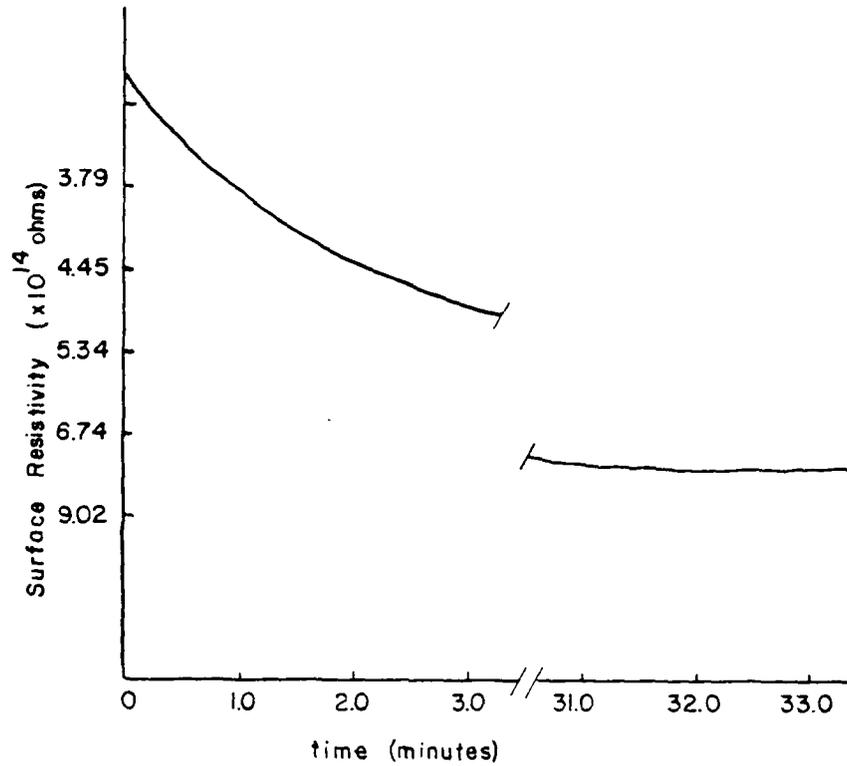
Figure 12-4 Surface resistivity of Nylon (2.5" diameter by .25" thickness) at 500 volts.
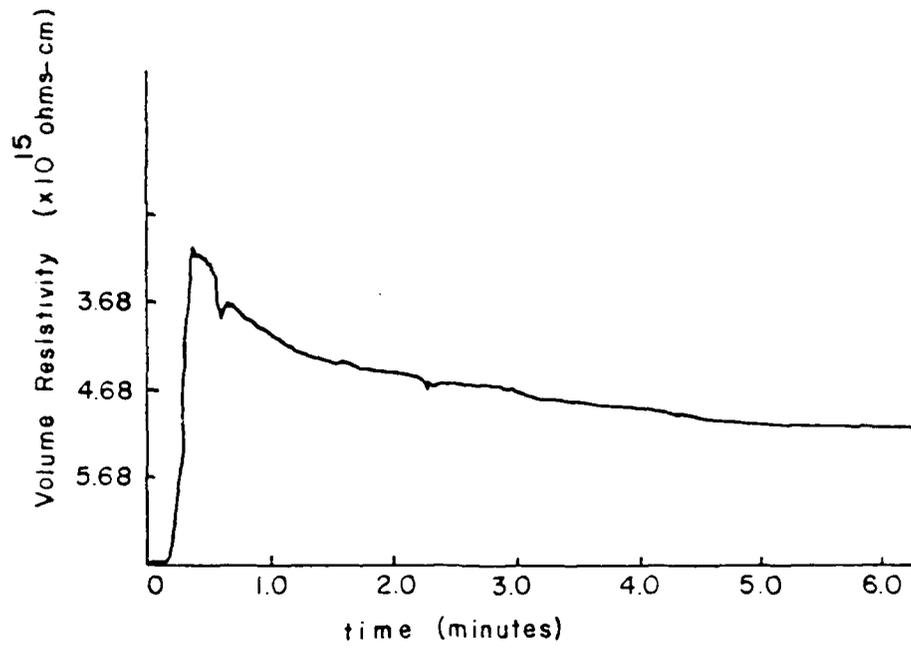
Figure 12-5 Volume resistivity of Nylon (2.5" diameter by
.25" thickness) at 500 volts.
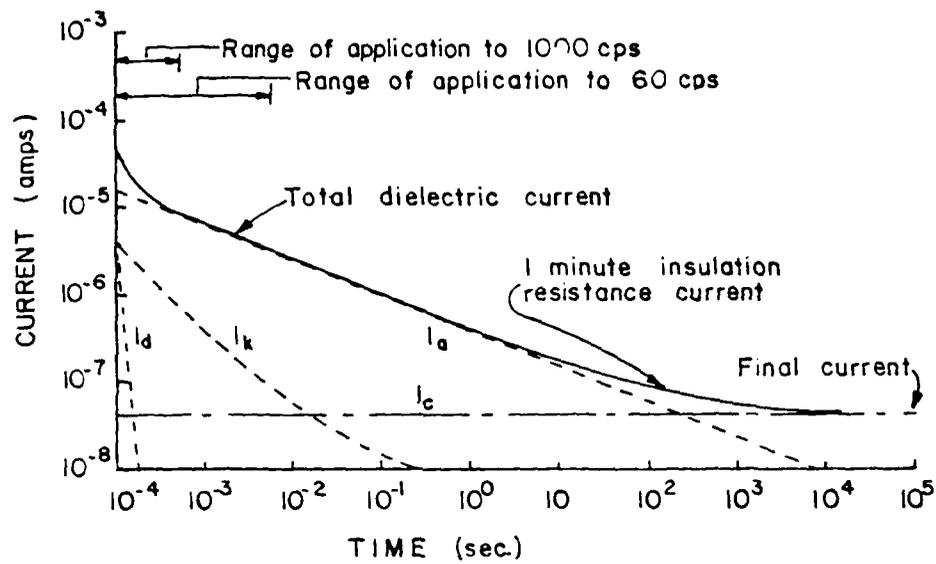
Figure 12-6 Currents as a function of time along an insulator
surface. I_d = charging current, I_a = reversible
absorption current, I_k = irreversible absorption current,
I_c = leakage conduction current. (ref. 5).

ity of a material is measured for a 1-minute electrification period.

Another serious problem in the measurement of resistivities is that temperature and humidity changes greatly effect the measured values. Fig. 12-7 shows the effect temperature has on the measurement of resistivity. These temperature and humidity variations are significant. Small changes in the temperature result in 25 to 50 percent changes in resistivity.

The shape of the samples used in our lab has been chosen to optimize measurement of the flashover potential. The dimensions are not compatible with the Keithley Model 6105 Resistivity Adapter and therefore a new instrument has been designed. Fig. 12-8 shows a resistivity adapter which we now have in our laboratory.

In our laboratory we irradiate insulating materials with ultraviolet radiation, and measure the resistivities afterwards. The point is to observe any changes in the resistivity because of surface damage. These changes will then be correlated with other data on the surface damage effects. At least the surface resistivity serves as a monitor on the damage. At best, some insight into surface charging problems may be obtained.

114
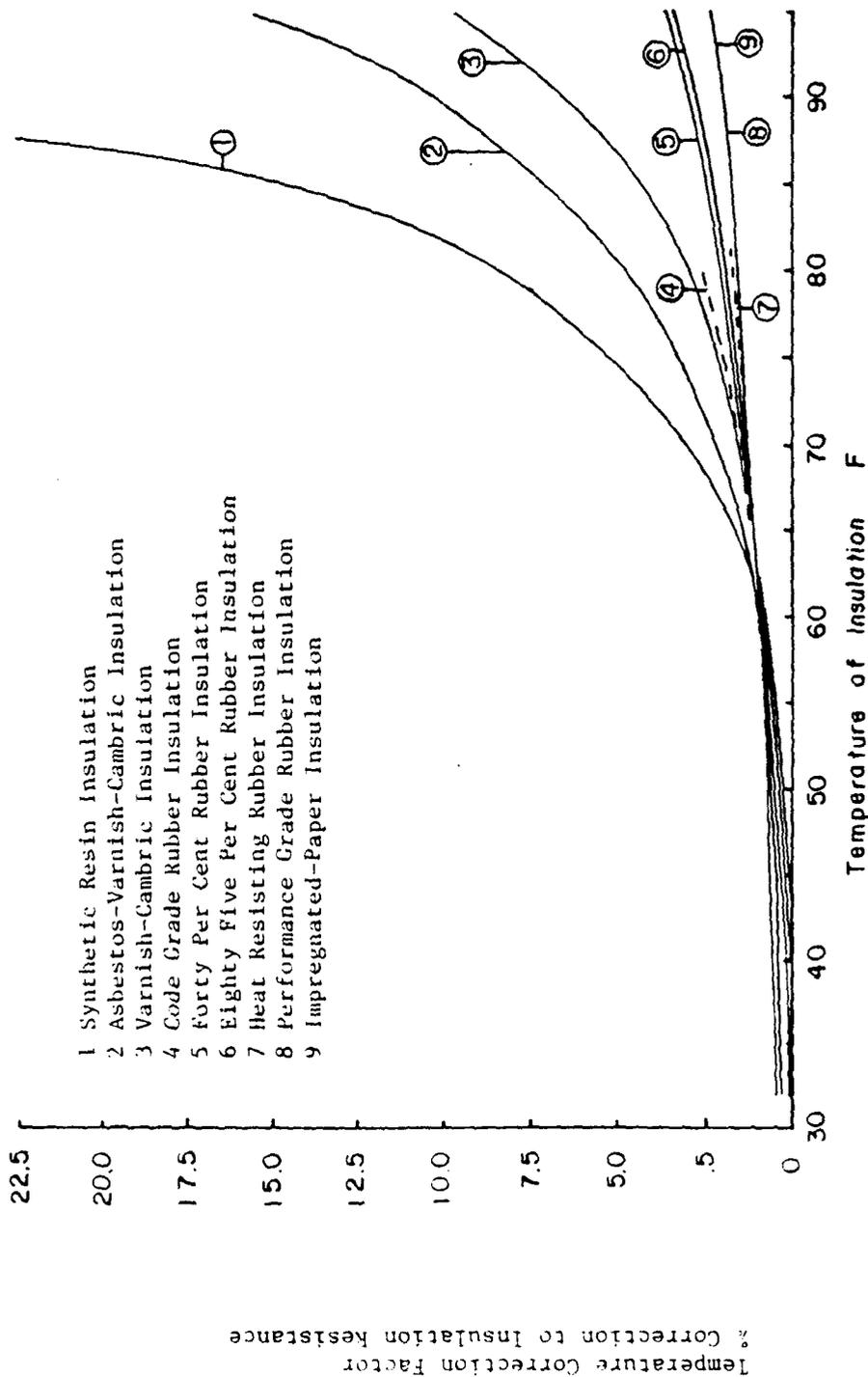
Figure 12-7 Temperature correction factors for various types of insulation.

1 Synthetic Resin Insulation
2 Asbestos-Varnish-Cambric Insulation
3 Varnish-Cambric Insulation
4 Code Grade Rubber Insulation
5 Forty Per Cent Rubber Insulation
6 Eighty Five Per Cent Rubber Insulation
7 Heat Resisting Rubber Insulation
8 Performance Grade Rubber Insulation
9 Impregnated-Paper Insulation

Temperature of Insulation F

Temperature Correction Factor
% Correction to Insulation Resistance

Figure 12-8 Top view of surface resistivity adapter

LIST OF REFERENCES

1. R. A. Anderson and J. P. Brainard, "Surface Flashover Model Based
    on Electron-Stimulated Desorption," Proceedings of VIII International
    Symposium on Discharge and Electrical Insulation in Vacuum,
    Albuquerque, New Mexico, 1978, D4.

2. P. A. Chatterton and D. K. Davies, "Secondary Electron Emission
    Characteristics of Insulator Surfaces Before and After Impulse
    Flashover," Proceedings of VIII International Symposium on Dis-
    charge and Electrical Insulation in Vacuum, Albuquerque, New
    Mexico, 1978, D2.

3. C. H. deToureil and K. D. Srivastova, "A Study of the Electrical
    Charging of the Surface of Insulation in Vacuum," Proceedings of
    the V International Symposium on Discharge and Electrical Insula-
    tion in Vacuum, Poland, 1972, 295.

4. H. C. Miller and E. J. Furno, "The Effect of Mn/Ti Surface Treat-
    ment on Voltage-Holdoff Performance of Alumina Insulators in
    Vacuum," Journal of Applied Physics, 49, 5416, (1978).

5. E. W. Greenfield, "Insulation Resistance Measurements," Electrical
    Engineering, July (1947), 698.

Chapter 13

Ellipsometry

Ellipsometry is a non-destructive optical technique through which information about the surface of a material may be obtained. The parameters measured can be related to the optical constants of the surface provided some information about the surface is available from another source. The problem of interpretation of the measured parameters is sufficiently complex that data from a completely unknown sample cannot be interpreted at all.

There are two reasons for the interest in ellipsometry for application to pulsed power problems. First, the technique is available for use in the laboratories at Texas Tech University. This means that samples can be analyzed quickly for an initial determination of changes in the surface. A sample that shows no damage could, for example, be sent back for more aging in a spark gap. Ellipsometry, therefore, plays the role of a monitor.

The second reason is that this technique is non-destructive. Almost all other surface analysis techniques require surface contact with a physical object, or the use of charged particles or x-ray beams as a probe. If the ellipsometric data later (after application of some other technique) gives some information on surface damage, that damage was present before the use of the other technique.

In the ideal ellipsometric measurement, a beam of monochromatic light is reflected from the surface of the sample of interest. The incident beam is prepared with components polarized both parallel and perpendicular to the plane of incidence. The composition of the reflected

beam is then analyzed. Two things can be measured for each polarization component of the incident and reflected waves; the phase angle of the component relative to some standard and the amplitude of the components. For ease of measurement and interpretation these quantities are usually combined to produce two measured parameters Ψ and Δ defined as follows:

$$\Psi = \tan^{-1}[\frac{R_p}{R_s} \frac{E_s}{E_p}]$$

$$\Delta = (\beta_p - \beta_s)_r - (\beta_p - \beta_s)_i$$

where

R is the amplitude of the reflected beam

E is the amplitude of the incident beam

β is the phase angle of the particular component

p used as subscript indicates the polarization component in the plane of incidence.

s used as a subscript indicates the polarization component perpendicular to the plane of incidence.

r, i used as subscripts indicate reflected and incident beams, respectively.

These two parameters are then used to write the equation of ellipsometry:

$$\frac{r_p}{r_s} = (\tan\Psi)\, e^{i\Delta}$$

where r denotes the reflection coefficient for the p or s component for the surface under study. The r can, in principle, be calculated using Fresnel's equations, however, this requires some knowledge of the surface. The ellipsometric measurement will give two parameters associat-

ed with the surface, for example the real and imaginary parts of the index of refraction, provided the other parameters entering Fresnel's equations are known. This is convenient for a surface which comprises the boundary between air and an optically flat homogeneous solid material. For an oxide film on a metal surface, however, there are five parameters; the real and imaginary parts of the indices of the oxide and the metal and the thickness of the film. Interpretation of the ellipsometric measurements thus requires either previous knowledge of the surface (a prepared sample) or the use of some other analysis technique to measure some of the parameters.

The purpose of this brief outline of the theory of ellipsometry is to indicate what kinds of information may be obtained using this technique. Detailed discussions of the theory appear elsewhere in the literature[1]. It is sufficient for our purpose to point out that if the index of refraction, n, and the extinction coefficient, k, can be measured by measuring Ψ and Δ, then the absorption coefficient α and the dielectric constant ε can be obtained from the following equations:

$$k = \frac{\alpha\lambda}{4\pi}, \quad \tilde{n} = n(1+ik), \quad \tilde{n} = \frac{\mu\tilde{\varepsilon}}{\mu_o \varepsilon_o}$$

where,

λ is the wavelength of the light

$\tilde{n}$ is the complex index of refraction

$\tilde{\varepsilon}$ is the complex dielectric constant of the sample

μ is the permeability of the sample

μ_o, ε_o are the permeability and permittivity of free space.

Fig. 13-1 is a schematic representation of the Gaertner L-119 ellipsometer used in the laboratory at Texas Tech University. This ar-
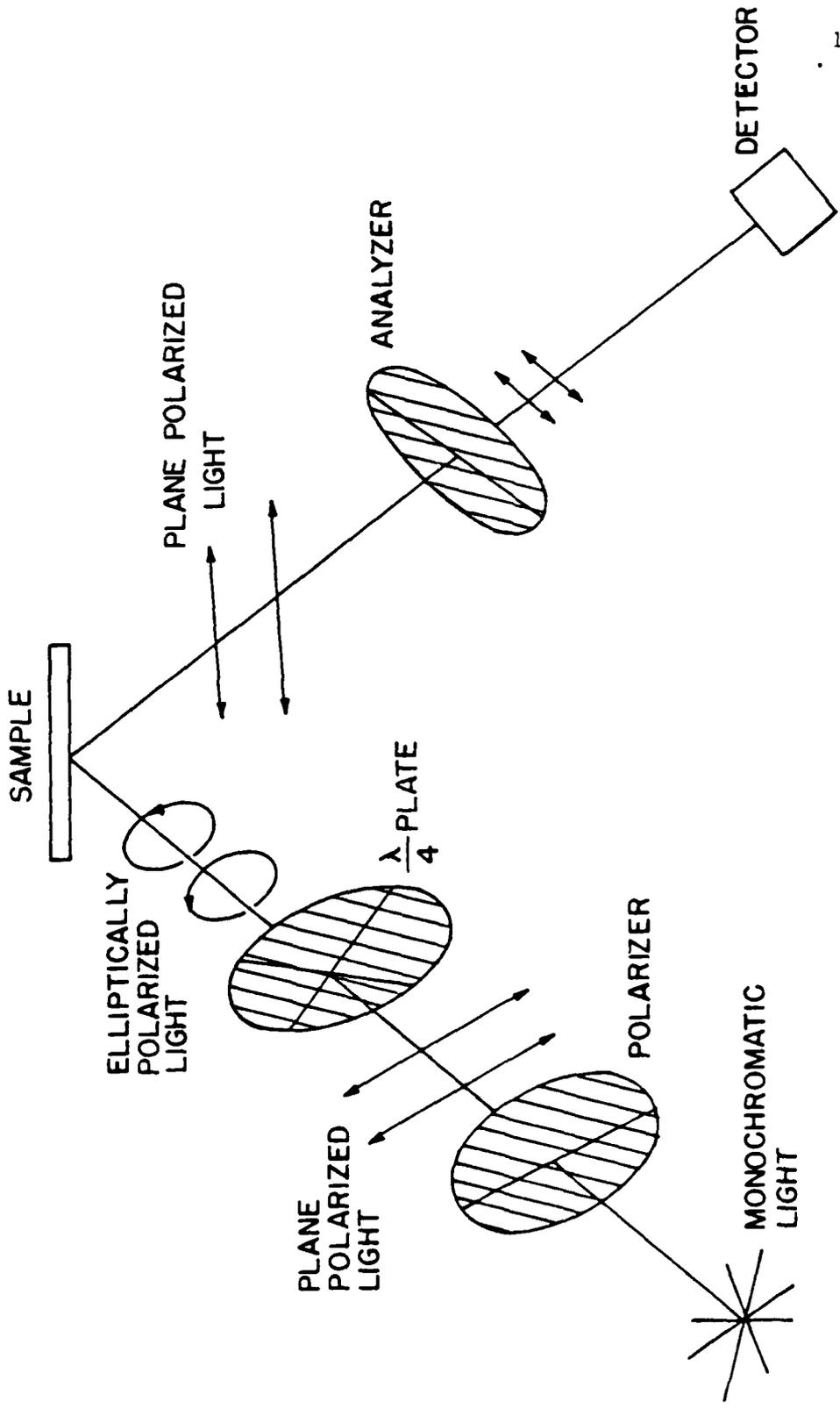
FIGURE 13-1

CONFIGURATION OF ELLIPSOMETER

ARCHER'S METHOD

rangement of components is known as Archer's method[2]. An incandescent lamp and monochromator are used to produce monochromatic light with a wavelength centered at 5461 Å. This beam is rendered plane polarized by the first polarizer (a Glan-Thompson prism) and elliptically polarized by the quater-wave plate, which is also called the compensator. The light reflects from the sample producing a change in the ellipticity which is then analyzed by a second polarizer identical to the first. A photomultiplier detects the light passing through the analyzer. This particular setup has been modified to include a chopping wheel and reference source between the monochromator and the ellipsometer. This allows the use of phase sensitive detection on the photomultiplier output signal.

Alignment and calibration of the machine is a lengthy process described in detail elsewhere[3]. Measurements of the two parameters Ψ and Δ are obtained by adjusting the two polarizers and the compensator for a null signal from the photomultiplier. The null detection can be made quite sensitive so that the accuracy depends on the precision with which the angles of the polarizers and compensator can be read. For the Geartner L-119 this is $\pm 0.01°$, leading to an accuracy of 100 ppm for the index of refraction of a material under ideal conditions.

The application discussed here is to detect changes in the surface of an insulating or conducting material that has been damaged in a spark gap. The advantages of ellipsometry are that it can be applied to large samples (~30 cm^2 surface area), is nondestructive, and is readily available in our laboratory. The disadvantage is that the data cannot be interpreted if little is known about the damaged surface.

For example, one must know either how deep the damaged layer is, or the index of refraction of the damaged layer, if there is an evaporated metal film on the surface, is the metal film oxidized, how thick are the films, etc.?

The samples analyzed in our laboratory by ellipsometry are then sent out for analysis by other techniques, such as AES or ESCA, to provide the answers to the above questions. Until quantitative information is available from outside testing, the ellipsometric data will be used only as a monitor of cumulative damage on a surface. Changes in the optical constants of a surface may not be a linear indicator of the amount of surface damage, however, in which case it would be valuable to establish the trends as an aid to further work.

Fig. 13-2 shows a schematic representation of the gas filled spark gap used to damage dielectric samples. This spark gap self breaks at about 35 kV when filled with air at atmospheric pressure. The air flow is set to change the gas in the chamber once for every breakdown. The energy passed by the gap during each spark is about 1200 J. The number of sparks to be administered to the samples is preset on an automatic counter which turns off the charging power supply at the end of the count.

The samples, which are about 4x8x.65 cm, are placed in the gap so that they stand parallel to the spark and about 4 cm distant from the spark. Different materials are treated at the same time.

Table 13-1 shows ellipsometric results for Lucite, delrin, and nylon. The samples were measured before the spark gap treatment and then subjected to 100 sparks. Different samples of the same materials were

GAS IN   GAS OUT

SAMPLES

H.V.   R

.25 Ω

$2 \mu f$

$10^3 : 1$

OSCILLOSCOPE

COUNTER
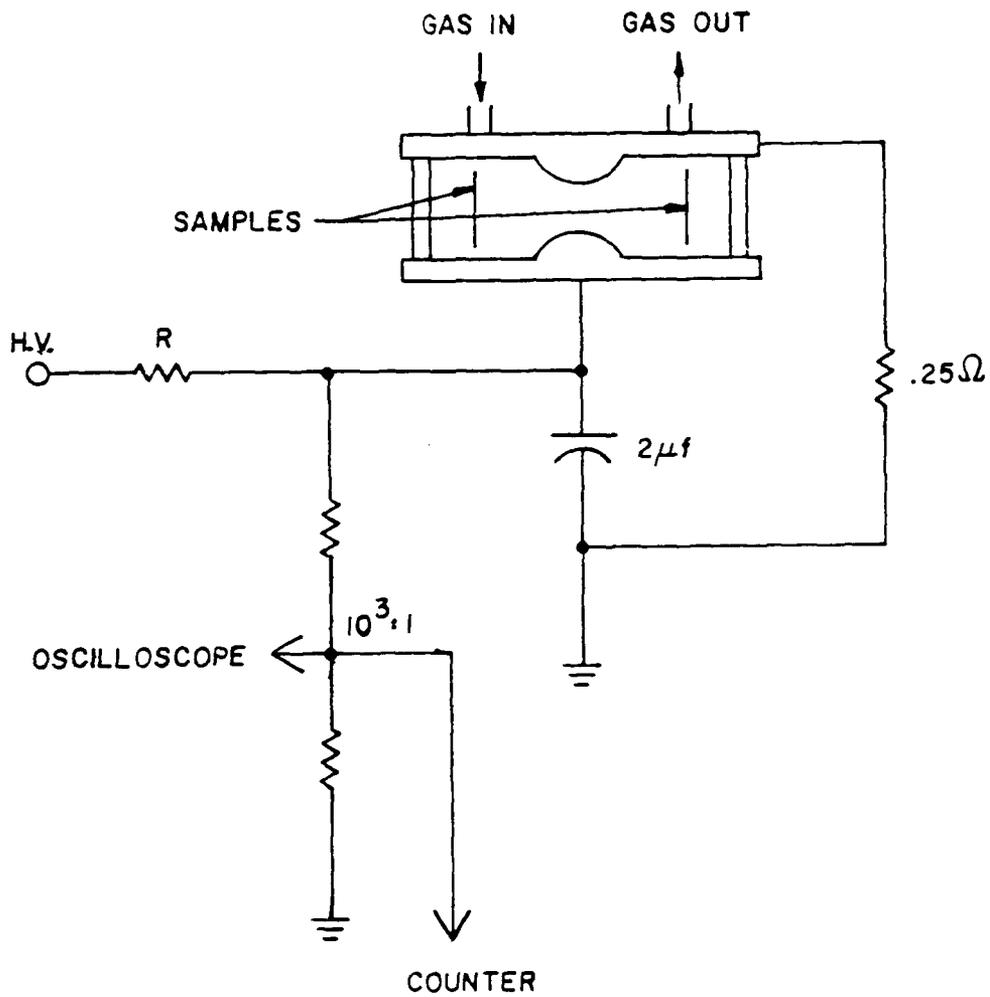
FIGURE 13-2

GAS FILLED SPARK GAP
USED TO DAMAGE INSULATORS

Table 13-I

		n	k
Undamaged	Spot 1	1.4916	0.0084
Lucite	Spot 2	1.4920	0.0085
Damaged	Spot 1	1.5980	0.0156
Lucite	Spot 2	1.6048	0.0153
(100 sparks)	Spot 3	1.6037	0.0153
Damaged	Spot 1	1.6228	0.0402
Lucite			
(100 sparks)			
Undamaged	Spot 1	1.4785	0.0077
Delrin	Spot 2	1.4785	0.0078
Damaged	Spot 1	1.6415	0.0585
Delrin	Spot 2	1.6453	0.0715
(100 sparks)			
Undamaged	Spot 1	1.5391	0.0364
Nylon	Spot 2	1.5410	0.0359
Damaged	Spot 1	1.3442	0.0817
Nylon	Spot 2	1.3082	0.0755
(100 sparks)			

then subjected to 1000 sparks. Visual inspection of the samples reveals obvious darkening and on the 1000 spark samples, the surface also appears to have been roughened. Since no more information is available about the damaged surfaces the model assumed for calculation is simply an air to single component solid interface.

Using this model, the index of refraction n and extinction coefficient k are calculated from the measured ellipsometric parameters. The calculation is performed using a computer code published by F. L. McCrackin[4]. The results are correct only if the simple model assumed is correct. The results shown in Table 13-1 are uncertain in the 4th decimal place for the undamaged samples and the samples subjected to 100 sparks. The lucite samples subjected to 1000 sparks apparently have a metal film which may be oxidized on the surface. This introduces a large uncertainty into the measurement. Also, these numbers may not have any meaning because of the simple model employed.

The trend of the numbers in Table 13-1 is that the absorption increases as the samples are subjected to more spark damage and the index of refraction increases or decreases depending on the material. These preliminary measurements are not sufficient to establish the trends but do indicate that ellipsometry may be useful as a damage monitor.

LIST OF REFERENCES

1. R. M. A. Azzam and N. M. Bashara, Ellipsometry and Polarized Light, (North Holland Publishing Company, New York, 1979).

2. R. J. Archer, Manual on Ellipsometry, (Gaertner Scientific Corp., Chicago, 1966).

3. F. L. McCrackin, E. Passalia, R. D. Stromberg, and H. L. Steinberg, "Measurement of the Thickness and Refractive Index of Very Thin Films and Optical Properties of Surfaces by Ellipsometry," Journ. Res. NBS, 67A, (1963).

4. F. L. McCrackin, "A Fortran Program for Analysis of Ellipsometric Measurements," Tech. Note No. 479 NBS, U. S. Governement Printing Office (1969).

Chapter 14

CONCLUSION

Now that the characteristics of some of the most common tech-
niques have been discussed, a criterion for the use of one or more of
the techniques will be given. Also, a review of the experimental work
being carried out in this laboratory will be given. For a surface an-
alysis technique to be useful it should possess some of the following
properties:

1) a surface analysis technique should be able to detect all ele-
   ments in a sample as well as changes in the chemical environ-
   ment;

2) it should also have an analysis depth of approximately 0-500
   $\overset{\circ}{A}$, in order to detect any changes in the chemical environ-
   ment caused by the various damage mechanisms;

3) it should have the sensitivity to detect small trace amounts
   of an element in a sample;

4) it should have enough resolution so that the analysis of the
   spectrum is straightforward;

5) it should be applicable to all kinds of samples, e.g. rough
   surfaces, conductors, and insulators;

6) the incident radiation should have no influence on the surface
   to be analyzed;

7) the sensitivity for detection of all elements should be about
   the same;

8) it should give absolute quantitative analysis.

Table 14-1 shows a comparison of the techniques which have been discus-

TABLE 14-1

Comparison of Various Surface Analysis Techniques

Technique	Primary Radiation Characteristics			Secondary Radiation Characteristics	
	Incident Radiation	Energy	FWHM	Analyzed Radiation	FWHM
ESCA	x-ray photons	1254 eV 1487 eV	.70 eV .85 eV	Secondary electrons	1-2 eV
AES	electrons	3 keV		Auger electrons	2-10 eV
SIMS	heavy ions	1-10 keV		Secondary ions	.1-5 eV
ISS	light ions	100 eV-1 MeV		Backscattered ions	
PAS	light			Acoustical waves	
ATR	light			Reflected light	
XRF	x-rays or electrons	10-100 keV		Characteristic x-rays	1-10 eV
SEM	electrons	1-10 keV		Secondary electrons, characteristic x-rays, Auger electrons	1-10 keV
SIPS	ions or neutrals	4 keV		Photons from excited backscattered ions or neutrals	2 Å

Technique	Analysis depth	Advantages	Disadvantages
ESCA	40-100 Å (insulators) 5-25 Å (conductors)	elemental analysis, nondestructive, core electron binding energy shifts give chemical analysis	complex spectrum with both Auger and photoelectron peaks
AES	40-100 Å (insulators) 5-25 Å (conductors)	elemental analysis, valence electrons give chemical information	destructive, complex spectrum, analysis of insulators is not well understood because of surface charging.
SIMS	5-25 Å	elemental analysis, detection of isotopes	destructive, neutralization processes not well understood.
PAS	2×10^{-3} cm	optical absorption data, analysis of all types of structures is possible	analysis depth is too great for present studies.
ATR	7000-10000 Å	optical absorption data	analysis depth is too great for present studies
XRF	1-2 μm	elemental analysis, nondestructive	fluorescence yields makes organic

Technique	Analysis depth	Advantages	Disadvantages
XRF (continued)			insulator analysis difficult, analysis depth is too great for present studies
SEM	5-100 Å 1-2 μm 5-100 Å	versatility	
SIPS	5-25 Å	insulator charging, problems decreased by use of neutrals, elemental analysis	processes are extremely complicated

sed.

The table gives information on the types of radiation used for the analysis as well as the analyzed radiation. The analysis depth is perhaps the most important characteristic of the analysis technique. Since the depth of damage in insulators caused by the various mechanisms in high voltage spark gaps is approximately 500 $\overset{o}{A}$, any analysis technique which gives information from greater depths is not applicable to the analysis of these insulators. For analysis of the insulators used in spark gaps the only techniques which meet this requirement are ESCA, AES, SIMS, and ISS. However, AES suffers from the problem of negative surface charging due to the use of electrons as the incident radiation. SIMS and ISS are both highly destructive and the ionization and sputtering processes involved in these techniques are not well understood.

ESCA is perhaps the only surface analysis technique capable of giving information about the changes and/or damage to insulators. It can detect all elements present in a sample, except hydrogen and helium, and it is capable of detecting changes in the chemical environment of atoms in insulators as shown by D. T. Clark, et. al. Also, the analysis of insulators by the use of x-rays does little damage to the surface during the analysis time. In other techniques, that use electrons or ions as the probing beam, the surface is damaged during the analysis.

The analysis of conductors is not hampered by surface charging problems. Consequently, the use of almost any technique is suitable for the analysis of conductors. Since ESCA, AES, SEM, and XRF are all well understood analysis techniques for the investigation of conductors,

these will be the primary analysis techniques for the conductors being investigated in the pulsed power laboratories at Texas Tech University.

One of the basic goals of this experiment is to differentiate between the various mechanisms which damage the insulators used in high voltage spark gaps. Because of this a vacuum system has been built in which the damage caused by ultraviolet radiation is isolated from the damage caused by other mechanisms, such as, the implantation of micro-particles from the electrodes, or heat from the high voltage discharge.

The vacuum system is composed of a 6 inch Varian diffusion pump, which typically produces a pressure of 10^{-7} Torr. A six inch gate valve is used to isolate the radiation chamber from the diffusion pump. This allows easy removal of the samples from the chamber. Fig. 14-1 shows a schematic of the vacuum system and various other components of the experiment. The ultraviolet radiation source is a surface discharge ignitor plug for a gas turbine engine which fires when the external spark gap fires. The external spark gap fires when the voltage, produced by charging a 750 pf capacitor to 20 kV through a 500 MΩ resistor, is sufficient to cause breakdown of the gap. The radiation produced by this ignitor plug is measured by a spectroradiometer located behind the MgF$_2$ window, which is transparent to ultraviolet radiation down to 2000 Å. This spectroradiometer measures the intensity versus wavelength of the radiation.

To insure that the samples are uniformly irradiated on all sides by the ignitor plug a D. C. motor is used to rotate the samples 180°. A photodiode counts the number of sparks from the ignitor plug. The output of the photodiode is connected to a counter which rotates the
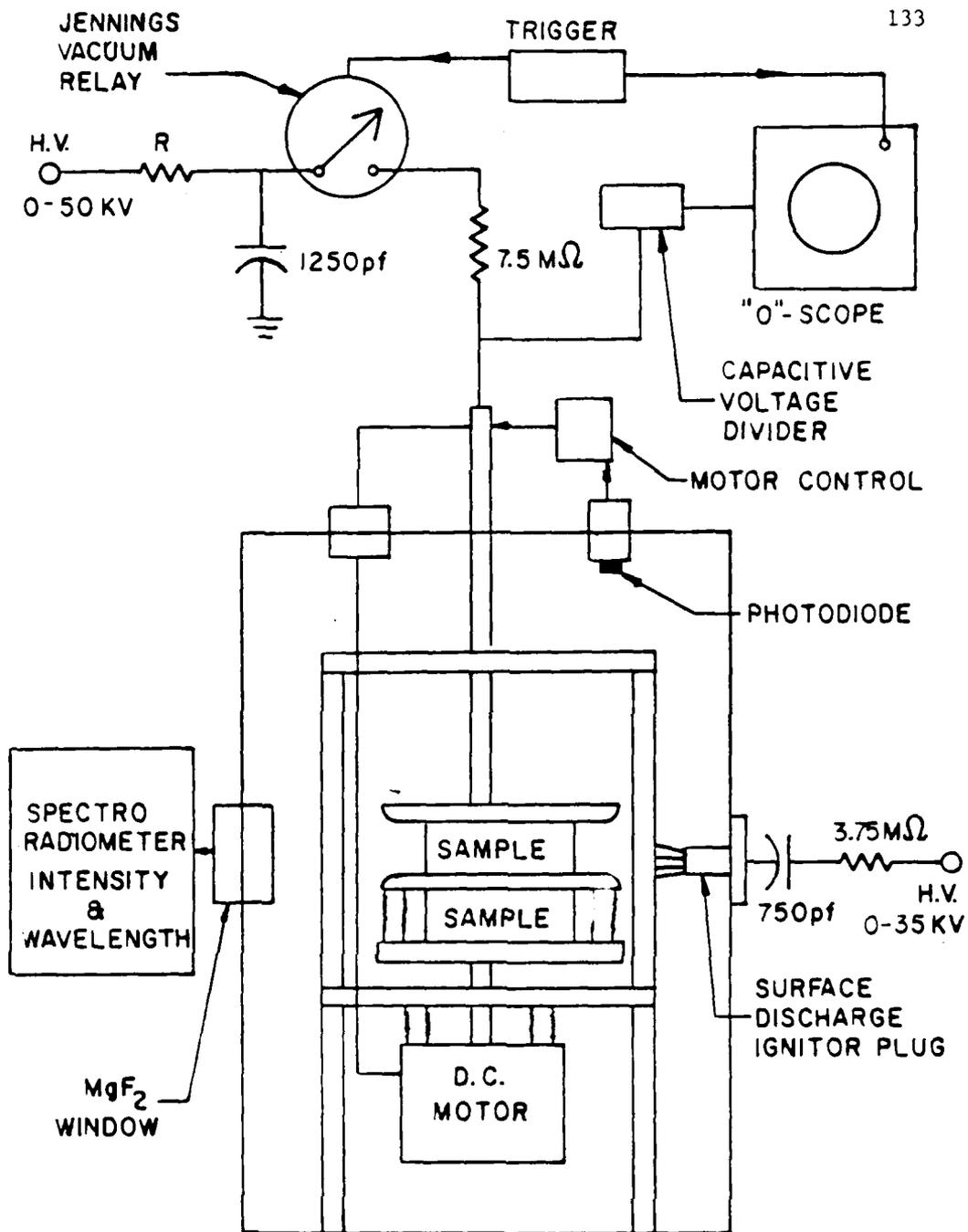
Figure 14-1

U-V Irradiation Chamber

samples when a predetermined number of sparks has been counted.

Before the samples are placed in the vacuum chamber the surface and volume resistivities of the samples are measured. The samples are then placed in the vacuum chamber and the breakdown voltage of the samples is measured. The surface flashover potential is measured by charging the two parallel plate uniform field electrodes (which make up approximately a 37 pf capacitor) through a resistor, the value of which determines the charging rate. A 7.5 MΩ resistor results in an exponential charging period of about 200 us. During some preliminary measurements of the flashover potential it was observed that a .5 inch Nylon sample broke down at 42 kV in 250 us. After the samples are irradiated by the ignitor plug the flashover potential is measured again. The two separate values of the flashover potential will be compared and related to the amount of radiation received by the samples. Hopefully a correlation between the amount of radiation received by the samples and the flashover potential can be observed. Also, measurements of the surface and volume resistivities will be performed and compared to the values of these quantities before the samples were irradiated.

These same samples will be sent off to some other research facility where they will be analyzed with an appropriate surface analysis technique.

ATE
MED
-8